

## Description of strongly coupled Yukawa fluids using the variational modified hypernetted chain approach

G. Faussurier\*

*Département de Physique Théorique et Appliquée, CEA/DAM Ile-de-France, Boîte Postale 12-F-91680, Bruyères-le-Châtel, France*

(Received 31 October 2003; published 2 June 2004)

The variational modified hypernetted chain approach as proposed by Rosenfeld [J. Stat. Phys. **42**, 437 (1986)] is used to describe strongly coupled Yukawa fluids. The integral equations of interest can be solved using the spherical harmonic oscillator wave functions as a seed. Comparisons are done with simulation results for equation of state and transport coefficients over the entire fluid domain for a wide range of the system parameters.

DOI: 10.1103/PhysRevE.69.066402

PACS number(s): 52.25.Fi, 52.25.Kn, 52.27.Gr

### I. INTRODUCTION

The physics of strongly coupled, screened Coulomb system is of great interest in many quite disparate fields such as dusty plasmas in connection with astrophysics and lithographic applications [1], dense stellar material and inertially confined plasmas [2,3], “mesoscopic plasmas” of charged-stabilized colloidal suspensions [4–6], or ultracold plasmas [7,8]. In the case of dusty plasmas, for instance, recent laboratory experiments have shown that the interparticle potential of charged dust particles in a plasma is given by the Yukawa potential with high accuracy in the absence of plasma flows [9]. Moreover, dusty (colloidal) plasmas are normal plasmas that achieve strong coupling with micron-sized impurities that can acquire  $10^3$  elementary charges. Indeed, dilute systems are relatively easy to produce and diagnose experimentally. This explains why dusty plasmas show great promise for studying the static and dynamic properties of strongly coupled, screened Coulomb systems over a wide parameter range. As a consequence, an extensive and intensive investigation of thermodynamics and transport coefficients for the three-dimensional (3D) Yukawa fluid is a topic of present considerable concern in dusty plasma physics.

Of course, in actual dusty plasmas, dynamics of charged dust particles can be more complex and subject to several other forces, such as collisions with background neutral gases. Here, our focus is on thermodynamics and transport properties in the absence of damping by background species. The Yukawa model therefore may be used as a simplified model for charged dust particles in a plasma, on which one can construct more realistic models to represent actual dusty plasmas under various conditions. However, the Yukawa system may also be of special interest as a mathematical model for many-body systems since it allows the full range of behavior between systems governed by short-range and long-range forces. For example, the Yukawa system is known as the one-component plasma (OCP) in the absence of screening. The OCP represents a system of ions when electrons are extremely mobile. The OCP has often been used as a classical model for the dense interiors of white dwarfs, where ions

are freely interacting with each other through Coulomb potentials in degenerate electron backgrounds. As the screening increases, the system acquires more characteristics of charge neutral fluids.

Screened Coulomb systems are frequently modeled with the Yukawa (Y) interparticle interaction of the form

$$v_Y(r) = \frac{Z^2 e^2}{r} \exp(-\alpha r). \quad (1)$$

Here,  $e$ ,  $Z$ , and  $\alpha$  are the electron charge, the ion charge, and an effective inverse screening length, respectively. If we express all lengths in units of Wigner-Seitz radius  $a_{WS}$ , the interparticle pair interaction  $v_Y$  times the inverse temperature  $\beta$  can be read under a more usual and compact expression

$$u_Y(r) = \frac{\Gamma}{r} \exp(-\kappa r), \quad (2)$$

where  $\Gamma = \beta Z^2 e^2 / a_{WS}$  and  $\kappa = \alpha a_{WS}$  are dimensionless coupling and screening parameters,  $\beta = 1/k_B T$ ,  $(4\pi/3)a_{WS}^3 \rho_i = 1$ .  $\rho_i = N/\Omega$  is the particle density of the system of  $N$  ions contained in the volume  $\Omega$ ,  $T$  is the temperature of the system supposed to be in thermodynamic equilibrium, and  $k_B$  is the Boltzmann constant. For dusty plasmas, the coupling refers to the dust grains and the screening to the hot background electron-ion plasma. For ultracold plasmas, the coupling refers to the cold ions and the screening to the partially degenerate electron gas. Similar arguments hold for other situations.

In short, the Yukawa system is simply a one-component plasma model constituted of a neutral classical plasma made of  $N$  identical point charges  $Z$  (ions) immersed in a uniform neutralizing background (electrons) of volume  $\Omega$  and charge density  $-\rho_e = -Z\rho_i$ . The effective interaction  $\mathcal{H}_Y$  between ions due to the polarization background of electrons may be expressed as follows [10]:

$$\begin{aligned} \mathcal{H}_Y = & \frac{1}{2} \sum_{i \neq j} Z^2 v_\alpha(|\mathbf{r}_i - \mathbf{r}_j|) - \sum_i \int d^3 \mathbf{r} \rho_e Z v_\alpha(|\mathbf{r} - \mathbf{r}_i|) \\ & + \frac{1}{2} \int d^3 \mathbf{r} \int d^3 \mathbf{r}' \rho_e^2 v_\alpha(|\mathbf{r} - \mathbf{r}'|) + N\mathcal{E}, \end{aligned} \quad (3)$$

where  $v_\alpha(|\mathbf{r}|) = e^2 e^{-\alpha r} / r$  and  $i, j = 1, \dots, N$ . In the right-hand

\*Email address: gerald.faussurier@cea.fr

side of Eq. (3), the first term is the particle-particle interaction, the second one is the particle-background interaction, the third one is the background-background interaction, whereas the last term fixes the zero of energy with respect to the self-energy of a bare Coulomb charge:

$$\varepsilon \equiv \frac{1}{2} \lim_{r \rightarrow 0} [Z^2 v_\alpha(r) - Z^2 v_0(r)]. \quad (4)$$

The Yukawa one-component plasma (YOCP) model can be characterized by the couple of parameters  $\Gamma$  and  $\kappa$ . The OCP system is recovered for  $\kappa=0$ .

Thermodynamic and structural properties of the YOCP have been thoroughly studied by means of Monte Carlo (MC) simulations on the hypersphere [10], by equilibrium molecular dynamics (MD) simulations within periodic boundary conditions [11–13], and by variational methods based on the Gibbs-Bogolyubov inequality [14–16]. The liquid-solid phase boundary and reliable estimates of the free energy are thus available in a wide range of the system parameters  $\{\Gamma, \kappa\}$  [10–14]. By contrast, less is known about the dynamical properties of the YOCP and, in view of hydrodynamical simulations, valuable estimates of the transport coefficients of YOCP are clearly wanted.

Very recently, MD, variational methods using the known properties of the reference system [14], or approximate methods based on excess entropy [17,18] have been used to estimate self-diffusion [14,19], shear viscosity [14,20], and thermal conduction [14] of the YOCP fluid in a systematic manner over an extensive range of the system parameters. For completeness, Salin and Caillol [21,22] have presented molecular dynamics computations of the thermal conductivity and the shear and bulk viscosities of the YOCP. More intensive MD calculations should bring many more results for thermal conductivity and bulk viscosity over a wider range of the system parameters  $\{\Gamma, \kappa\}$  within the entire fluid domain in order to determine the principal transport coefficients of the YOCP completely.

One could thus think the problem of characterizing the main static and dynamic properties of the YOCP nearly solved. In fact, this is not the case for, at least, two main reasons. First, the static structure factor  $S(k)$  and the pair distribution function  $g(r)$  form the basic ingredients in nearly all theories describing strongly coupled regimes [23]. To study the excitation and propagation of waves, one needs the dynamical dielectric function. The latter is not easily determined in a strongly coupled plasma. An approximation scheme, however, referred to as QLCA (quasilocalized charge approximation) [24] has been successfully used for a variety of plasma systems [25], including strongly coupled dusty plasmas [26,27]. In this approach,  $g(r)$  is a key parameter that governs the behavior of the dynamical dielectric function. In the same spirit, the pair correlation function is known to play a key role in the APEX method of generating the electron ion microfield for use in the line shape formalism [28–31]. We must confess that MC or MD codes are not black-box algorithms and have not been designed to give a rapid access to  $g(r)$  and  $S(k)$  for computing time reason, whatever  $\Gamma$  and  $\kappa$  may be within the entire fluid domain

[32,33]. Furthermore, no simple analytic expressions exist for  $g(r)$  and  $S(k)$  of the YOCP that are precise, robust, and consistent with the equation of state determined from the MC or MD simulations. As for the variational method based on the Gibbs-Bogolyubov inequality [14], it is not clear if  $g(r)$  and  $S(k)$  of the reference system may be of particular utility in this context. This method is known to be well suited to estimate system free energy but great care is required when  $g(r)$  of the reference system is employed to calculate anything else than the free energy [14]. Second, the screening potential  $H(r)$  is a function of fundamental interest in strongly coupled plasmas because (i) the enhancement factors for the thermonuclear reaction rates, which are important for stellar evolution, are essentially controlled by the short-range part of the screening potential, (ii) the screening potentials play a key role in the study of the short-range behavior of the Bridge functions, notably their universal properties, which proved seminal for developing an accurate theory of liquid structure, and (iii) they offer consistency checks for the equation of state of a mixture and for closure approximation in integral equation theories for the fluid pair structure [3]. Again, this function is very difficult to extract from MC or MD simulations [34–38] and the variational method seems to have nothing to say concerning this topic. Something else should thus be done.

Fortunately, the integral equation theory for the pair structure of simple fluids, which was developed in 1950s and early 1960s [23], has been the subject of a strong interest during the last three decades [39–48]. Among many methods available in literature, the variational modified hypernetted chain (VMHNC) approach, as proposed by Rosenfeld [48], has been proven to be very accurate to describe the structure and thermodynamic properties of liquid metals by comparisons with molecular dynamics results [49–51]. Based on the approximation of universality of the Bridge function, the derivation of the VMHNC method ensures the thermodynamic consistency between the Helmholtz free energy and the virial routes to the equation of state. So doing, the energy and the virial pressure equations of state satisfy the Hiroike's test [52]. This consistency is also enjoyed by the hypernetted chain (HNC) approximation from where it originates but, unlike the HNC, the variational procedure ensures reasonably good thermodynamic consistency between the compressibility and the virial routes without enforcing it. Moreover, the VMHNC has the advantage of avoiding small, unphysical, structural deficiencies posed by the analytic behavior of the Verlet-Weiss-Grundke-Henderson [53,54] hard-sphere (HS) parametrized Bridge function used by Lado *et al.* [44]. A bootstrap procedure akin to the one introduced by Ross [55] to deal with the softness of the repulsive potential allows one to use directly the much better behaved Percus-Yevick (PY) Bridge function [56–58], without any resort to simulations. To sum up, the VMHNC method provides a simple, robust, and entirely first principles approach to the theory of the structure and thermodynamics of simple classical liquids based on a local (i.e., without the need to integrate along an isotherm or an isochore) free-energy functional that determines by variation both the structure and the equation of state. The VMHNC theory is free from any ad-

justable parameter and the energy-virial thermodynamic self-consistency is guaranteed without imposing it. To be complete, it can also be used to extract the potential from pair distribution function and/or structure factor obtained from experiment or quantum molecular dynamics simulations. In summary, this approach for calculating the pair structure for a given potential and for inverting structure factor to obtain the potential and the thermodynamic functions has no equivalent in the field of simple liquids.

In this paper, we propose to provide a benchmark test regarding the calculation of the complete equation of state, structure, and transport coefficients for the bulk YOCP fluid employing the VMHNC theory, with the general purpose of stimulating its quotidian use. This paper is a companion, both in scope and methods, to a recent general-purpose methodology to describe strongly coupled Yukawa fluids using the variational method based on the Gibbs-Bogolyubov inequality [14]. In Sec. II, the VMHNC is reviewed and applied to Yukawa system. A simple method is presented to deal with the long-range interaction. This method is consistent with and generalizes the original one proposed for the OCP system [59]. A technique is proposed to cope with the initialization of the HNC-like equations for strongly coupled cases. The general idea consists in rewriting and solving the HNC equations using a variational principle. The unknown function is the short-range direct correlation function. This function is expanded in the harmonic oscillator wave functions (HOF) [60] and the undetermined coefficients of the development are found minimizing a functional of interest. A limited number of HOF is sufficient to give a reasonable first guess to speed up the convergence of the HNC equations. Computational details are also given. In Secs. III and IV, we compare our results for thermodynamics and transport coefficients to the most recent, accurate, and extensive sets of simulation data presented by Hamaguchi *et al.* [11–13,19,20]. Section V is devoted to the pair correlation function, structure factor, and screening potential. Section VI is the conclusion.

## II. FORMULATION

Taking advantage of the universal character of the Bridge function [40], Rosenfeld constructed an effective excess free-energy functional  $F(\beta, \rho_i, \eta)$  that satisfies the virial-energy consistency criterion for a given pair potential  $\phi(r)$ . Then, making use of the Percus-Yevick hard-sphere Bridge function, the best free energy is determined by minimization with respect to the pair distribution function and to the packing fraction of the auxiliary hard-sphere system. The minimization with respect to the pair distribution function leads to the modified hypernetted chain equations (MHNC) [40], i.e., the standard integral equations of simple fluid theory, with the HS Bridge function expressed within the PY approximation replacing the exact but unknown Bridge function of the system under study. Minimization with respect to the packing fraction  $\eta$  leads to a criterion for its optimum choice involving the Bridge function  $B_{HSPY}(r, \eta)$  and the pair distribution function  $g_{HSPY}(r, \eta)$  of the HS system treated in PY approximation, the pair distribution of the MHNC equation  $g(r)$ , and

a necessary correction term; this term originates from using the HSPY Bridge function instead of the exact HS Bridge function. The corresponding recipe for calculating  $g(r)$  from given potential  $\phi(r)$ , temperature  $\beta$ , and density  $\rho_i$  reads as follows. Solve the MHNC equations using  $B_{HSPY}(r, \eta)$  for various values of  $\eta$ , i.e.,

$$h(r) = c(r) + \rho_i \int d\mathbf{r}' h(|\mathbf{r} - \mathbf{r}'|) c(r'),$$

$$\ln[g(r)] = -\beta\phi(r) + h(r) - c(r) + B_{HSPY}(r, \eta),$$

$$h(r) = g(r) - 1. \quad (5)$$

Monitor  $\eta$  until the excess free energy  $f_\phi^{VMHNC}(\beta, \rho_i, \eta) = \beta F(\beta, \rho_i, \eta)/N$  is minimum for some value  $\eta = \eta_{eff}$ , i.e.,

$$0 = \frac{d\delta_\phi(\eta)}{d\eta} - \frac{\rho_i}{2} \int d\mathbf{r} [g(r) - g_{HSPY}(r, \eta)] \frac{\partial B_{HSPY}(r, \eta)}{\partial \eta}, \quad (6)$$

with

$$\delta_\phi(\eta) = f_{CS}(\eta) - f_{PYV}(\eta) = \frac{\eta(4-3\eta)}{(1-\eta)^2} - \frac{6\eta}{(1-\eta)} - 2\ln(1-\eta). \quad (7)$$

Here,  $f_{CS}(\eta)$  and  $f_{PYV}(\eta)$  are the Carnahan-Starling (CS) and PY-virial (PYV) free energies, respectively. Once done, the pair correlation function is the solution of the MHNC equations with the Bridge function given by  $B_{HSPY}(r, \eta_{eff})$  and the excess free energy of the system is given by

$$\begin{aligned} f_\phi^{VMHNC}(\beta, \rho_i, \eta) &= \frac{\rho_i}{2} \int d\mathbf{r} g(r) [\beta\phi(r) - B_{HSPY}(r, \eta)] \\ &\quad - \frac{\rho_i}{2} \int d\mathbf{r} \left\{ \frac{1}{2} h(r)^2 + h(r) - g(r) \ln[g(r)] \right\} \\ &\quad - \frac{1}{2\rho_i} (2\pi)^{-3} \int d\mathbf{k} \{ \ln[1 + \tilde{h}(k)] - \tilde{h}(k) \} \\ &\quad + \delta_\phi(\eta) + \Delta_{PY}(\eta), \end{aligned} \quad (8)$$

with  $\eta = \eta_{eff}$  and where

$$\Delta_{PY}(\eta) = \int_0^\eta d\eta' \frac{1}{2} \int d\mathbf{r} g_{HSPY}(r, \eta') \frac{\partial B_{HSPY}(r, \eta')}{\partial \eta}. \quad (9)$$

Note that one may encounter authors, who consider the Bridge function to be either  $B_{HSPY}(r, \eta)$  or  $-B_{HSPY}(r, \eta)$ . The VMHNC can be applied to YOCP straightforwardly, with a careful treatment of the long-range Yukawa interaction, and with a slight modification of the excess free-energy expression due to background [i.e.,  $g(r)\beta v_Y(r)$  must be replaced by  $h(r)\beta v_Y(r)$ ] and energy reference (i.e.,  $\beta\mathcal{E}$  must be included). Since these questions are related, let us discuss the long-range question first. We will then give the resulting practical expression of the YOCP excess free energy within the VMHNC theory.

As well known, the MHNC equations are not easy to solve for strongly coupled Yukawa system for two main reasons. First, in the weak-screening limit, i.e.,  $\kappa \in [0, 1]$ , the more we approach the OCP limit, the less the Yukawa potential can be considered as short range. Since the direct correlation function  $c(r)$  is equivalent to  $-\beta\phi(r)$  when  $r \rightarrow \infty$ , the Fourier transform  $\tilde{c}(k)$  of  $c(r)$  cannot be calculated numerically. This prevents the inversion of the Ornstein-Zernike equation, i.e., the one-to-one map between  $\tilde{c}(k)$  and  $\tilde{h}(k)$ , and, as a consequence, the resolution of the MHNC equations. Second, in the limit of strong coupling, i.e.,  $\Gamma \gg 1$ , the more we approach the liquid-solid phase boundary, the slower is the convergence of the iterative process to solve the MHNC equations. Indeed, these equations form a highly nonlinear coupled set of equations, which is a rather non-trivial numerical problem to handle. The iterative scheme, even with a relaxation scheme, can suffer from slow convergence, oscillation, and instability [61]. Moreover, the MHNC equations have to be solved by constantly going back and forth between real and reciprocal spaces. This is due to the convolution product, and the arising Fourier transform brings additional numerical difficulties. Though some progress has been made in this field, there is still a need for a simple, rapid, and robust algorithm to solve MHNC equations, i.e., a black-box package that works for any  $\phi(r)$  of physical interest, given either analytically or by a set of two-column data point file. This question is far more crucial, for instance, when MHNC equations are coupled to self-consistent field equations to determine the electronic and ionic structures in warm and hot, correlated, dense plasmas [61]. The first issue is solved by extending to Yukawa system the method of Ng [59], while the second issue is assessed by looking for an approximate solution of the MHNC equations with a spectral-Galerkin-like method based on the 3D spherical HOF.

The method of Ng [59], originally proposed for OCP system, consists in mapping a long-range to a short-range system. As for YOCP, this can always be done by considering the Yukawa potential  $u_Y(r)$  as a sum of two terms, a short-range potential  $u_{Y,S}(r)$  and a long-range potential  $u_{Y,L}(r)$ . Due to the asymptotic behavior of  $c(r)$ ,  $-u_{Y,L}(r)$  can be considered as the long-range part of  $c(r)$ . It is thus natural to introduce the short-range part  $c_S(r)$ , such that

$$c(r) = c_S(r) - u_{Y,L}(r). \quad (10)$$

All the trick, then, is to have for  $u_{Y,L}(r)$  a function with an analytic Fourier transform, and a corresponding nonsingular and well-behaved  $c_S(r)$ , that can easily be Fourier transformed numerically. The simplest solution is to employ the method of Ng [59], i.e.,

$$\begin{aligned} u_{Y,L}(r) &= u_Y(r) \operatorname{erf}(\alpha_{NG} r), \\ u_{Y,S}(r) &= u_Y(r) \operatorname{erfc}(\alpha_{NG} r), \\ u_Y(r) &= u_{Y,L}(r) + u_{Y,S}(r), \end{aligned} \quad (11)$$

where  $\operatorname{erf}(\alpha_{NG} r)$  and  $\operatorname{erfc}(\alpha_{NG} r)$  are the error and complementary error functions

$$\operatorname{erf}(x) = \frac{2}{\sqrt{\pi}} \int_0^x e^{-t^2} dt, \quad (12)$$

$$\operatorname{erfc}(x) = 1 - \operatorname{erf}(x) = \frac{2}{\sqrt{\pi}} \int_x^\infty e^{-t^2} dt.$$

$\alpha_{NG}=1.08$  suggested by Ng [59] has been kept for YOCP too. We recall that with this value and  $\kappa=0$ ,  $u_Y(r)$  agrees to 99% or more with  $-c(r)$  over a wide range of values for  $r$  and  $\Gamma$ . Using  $\operatorname{erf}(\alpha_{NG} r)$  as a cutting function allows one to compute analytically the Fourier transform  $\tilde{u}_{Y,L}(k)$  of  $u_{Y,L}(r)$ , while ensuring the continuity of the treatment in the weak-screening limit with the OCP. The explicit expression of  $\tilde{u}_{Y,L}(k)$  is found after standard algebraic calculations and reads

$$\tilde{u}_{Y,L}(k) = \frac{4\pi\Gamma}{k^2} \operatorname{Re} \left[ \frac{k}{k+i\kappa} w \left( \frac{k+i\kappa}{2\alpha_{NG}} \right) \right], \quad (13)$$

where  $i$  is the complex number such that  $i^2=-1$  and  $\operatorname{Re}(z)$  means the real part of complex number  $z$ .  $w(z)$  involves the complex error function,

$$w(z) = e^{-z^2} \left( 1 + \frac{2i}{\sqrt{\pi}} \int_0^z e^{t^2} dt \right). \quad (14)$$

In practical calculation, we have used the FORTRAN routine `wwerf` from the CERN library `MATHLIB` [62,63]. We can check that the formula proposed by Ng [59] for OCP is recovered as a particular case when  $\kappa=0$ . With such a decomposition, the MHNC equations are easily solved since the Bridge function remains short range by essence. Now, the effective MHNC equations read in  $a_{WS}$  units

$$\begin{aligned} h(r) &= -u_{Y,L}(r) - \frac{3}{4\pi} \int d\mathbf{r}' h(|\mathbf{r}-\mathbf{r}'|) u_{Y,L}(r') + c_S(r) \\ &\quad + \frac{3}{4\pi} \int d\mathbf{r}' h(|\mathbf{r}-\mathbf{r}'|) c_S(r'), \\ \ln[g(r)] &= -u_{Y,S}(r) + h(r) - c_S(r) + B_{HSPY}(r, \eta), \end{aligned} \quad (15)$$

whereas

$$\begin{aligned} f_Y^{VMHNC}(\beta, \rho_i, \eta) &= \frac{\rho_i}{2} \int d\mathbf{r} [h(r) \beta v_Y(r) - g(r) B_{HSPY}(r, \eta)] + \beta \mathcal{E} - \frac{\rho_i}{2} \\ &\quad \times \int d\mathbf{r} \left\{ \frac{1}{2} h(r)^2 + h(r) - g(r) \ln[g(r)] \right\} - \frac{1}{2\rho_i} (2\pi)^{-3} \\ &\quad \times \int d\mathbf{k} \{ \ln[1 + \tilde{h}(k)] - \tilde{h}(k) \} + \delta_\phi(\eta) + \Delta_{PY}(\eta), \end{aligned} \quad (16)$$

using the MHNC equations, reduces to

$$\begin{aligned}
f_Y^{VMHNC}(\Gamma, \kappa, \eta) = & -\frac{\Gamma\kappa}{2} - \frac{3}{8\pi} \int d\mathbf{r} \left[ -\frac{1}{2}h(r)^2 - h(r)u_{Y,L}(r), \right. \\
& + g(r)c_S(r) + u_{Y,S}(r) \left. \right] - \frac{1}{12\pi^2} \int d\mathbf{k} \\
& \times \{ \ln[1 + \tilde{h}(k)] - \tilde{h}(k) \} + \delta_\phi(\eta) + \Delta_{PY}(\eta)
\end{aligned} \quad (17)$$

in  $a_{WS}$  units.

In order to speed up the resolution of MHNC equation in strong-coupling limit and stabilize the interactive convergent process, the short-range part  $c_S(r)$  of the direct correlation function is expanded in the 3D spherical HOF  $\{\varphi_n(r, \alpha_{HOF})\}$ , which form a complete basis for a given harmonic oscillator parameter  $\alpha_{HOF}$ :

$$c_S(r) = \sum_{n \geq 0} c_n \varphi_n(r, \alpha_{HOF}), \quad (18)$$

$$\begin{aligned}
\varphi_n(r, \alpha_{HOF}) \\
= \left[ \frac{n! (1/2)!}{(n+1/2)!} \right]^{1/2} \left( \frac{\alpha_{HOF}}{\pi} \right)^{3/4} L_n^{1/2}(\alpha_{HOF} r^2) e^{-\alpha_{HOF} r^2/2},
\end{aligned} \quad (19)$$

where  $\{L_n^{1/2}(x)\}$  are Laguerre polynomials,  $n! = \Gamma(n+1)$ , and  $(n+1/2)! = \Gamma(n+3/2)$ .  $\Gamma(z)$  is the  $\Gamma$  function, i.e.,  $\Gamma(z+1) = z\Gamma(z)$ , and should not be confused with the coupling parameter  $\Gamma$  of the Yukawa system. Since  $c_S(r)$  is finite, short range, and takes values small in magnitude for  $r$  between 0 and a few  $a_{WS}$ , only a finite and limited number  $N_{HOF}$  of HOF is sufficient to have a good starting point to solve the MHNC equations from scratch. For strong coupling, this seed is better than the simple guess  $c_S(r)=0$ . Note that this approach is local and is well suited to the general philosophy of the VMHNC theory. Moreover, there is less need to start from a closed solution with a smaller  $\Gamma$ , this nonlocal method having the drawback of requiring a painstaking, careful, and computer time consuming resolution of MHNC equations from small to the present value of  $\Gamma$ . There exist tremendous ways to expand a function upon a complete basis. We have chosen the 3D spherical HOF because they possess many advantages for numerical and physical purpose as well. Originally, they have been extensively used in nuclear physics to calculate two-body matrix elements within the Hartree-Fock-Bogolyubov theory combined with effective density-dependent interaction [60]. Their important properties can be summarized as follows. First, for a well-behaved and localized function [such as  $c_S(r)$  here], a limited number of terms of the series is needed to represent it. Moreover, the coefficients of the development are easily calculated by Gauss-Laguerre quadrature when such a function is known from outside [64]. Second, due to the properties of the associated generating functions, the Fourier transform  $\tilde{\varphi}_n(k, \alpha_{HOF})$  is simply related to  $\varphi_n(r, \alpha_{HOF})$  by the formula

$$\tilde{\varphi}_n(k, \alpha_{HOF}) = (-1)^n (2\pi)^{3/2} \varphi_n(k, 1/\alpha_{HOF}). \quad (20)$$

Third, the HOF satisfy the crucial theorem of separability, i.e., any product of HOF can be written as a finite sum of HOF. With this information in mind, the unknown coefficients  $\{c_n\}$  are determined by minimizing the following functional  $\mathcal{F}(c_n, \eta)$ , which is equivalent to the MHNC equations, at fixed  $\eta$  [65,66]:

$$\mathcal{F}(c_n, \eta) = \int d\mathbf{r} [1 + h(r) - e^{-u_{Y,S}(r)+h(r)-c_S(r)+B_{HSPY}(r, \eta)}]^2, \quad (21)$$

where

$$h(r) = \int \frac{d\mathbf{k}}{(2\pi)^3} \frac{\tilde{c}_S(k) - \tilde{u}_{Y,L}(k)}{1 - \rho_i[\tilde{c}_S(k) - \tilde{u}_{Y,L}(k)]} \quad (22)$$

and

$$\tilde{c}_S(k) = \sum_{n=0}^{N_{HOF}} (-1)^n c_n (2\pi)^{3/2} \varphi_n(k, 1/\alpha_{HOF}). \quad (23)$$

In practice, the MHNC equations are solved with  $N_{HOF}=5-10$  HOF at given  $\alpha_{HOF}=5$ . The approximate solution  $c_S(r)$  is then injected in the standard MHNC equation solver with relaxation scheme. Following Ng [59], we are using fast Fourier transform with real and reciprocal meshes with constant steps  $\Delta r$  and  $\Delta k$ ; 4096 mesh points are used,  $\Delta r = 50a_{WS}/4096$  and  $\Delta r \Delta k = \pi/4096$ . As for  $B_{HSPY}(r, \eta)$ , we have adopted the Baxter solution for the HSPY problem [24,58]. The exact HSPY expression of the pair distribution function is used for  $r$  between one and two times the HS diameter  $\sigma$ , in order to have a smooth junction around  $\sigma$  between the expression of  $B_{HSPY}(r, \eta)$ , based on the exact HSPY expression of the direct correlation function below  $\sigma$ , and the one based on the HSPY expression of the pair distribution function above  $\sigma$ .  $B_{HSPY}(r, \eta)$  is expanded in Chebyshev polynomials, with respect to both  $r$  and  $\eta$  variables, and tabulated. The calculations of  $\partial B_{HSPY}(r, \eta) / \partial \eta$ ,  $\delta_\phi(\eta)$ , and  $\Delta_{PY}(\eta)$  are then straightforward using the properties of the Chebyshev polynomials [64]. As noted by Perrot [67], the value of  $\eta$  obtained in the variational method using the Gibbs-Bogolyubov inequality and the HS system to describe YOCP is a very good starting point for solving the MHNC criterion. We have thus simply used the analytic fit for  $\eta$  in function of  $\Gamma$  and  $\kappa$  proposed in Ref. [14] [Eqs. (19)–(21)]. As for the minimization of Eq. (21), we have used the conjugate-gradient program suggested by Krauth and Staudacher [65].

Before closing this section, one must confess that we could have used the HOF directly within the expression of the excess free energy  $f_Y^{VMHNC}(\beta, \rho_i, \eta)$  and minimize it with respect to  $\{c_n\}$  and  $\eta$ , in the spirit of the VMHNC theory. Such a strategy is challenging but deserves a particular study, which is beyond the scope of this paper. Since our original idea was to simply have a seed to speed up the resolution of the MHNC equations, we have found  $\alpha_{HOF}=5$  highly suffi-

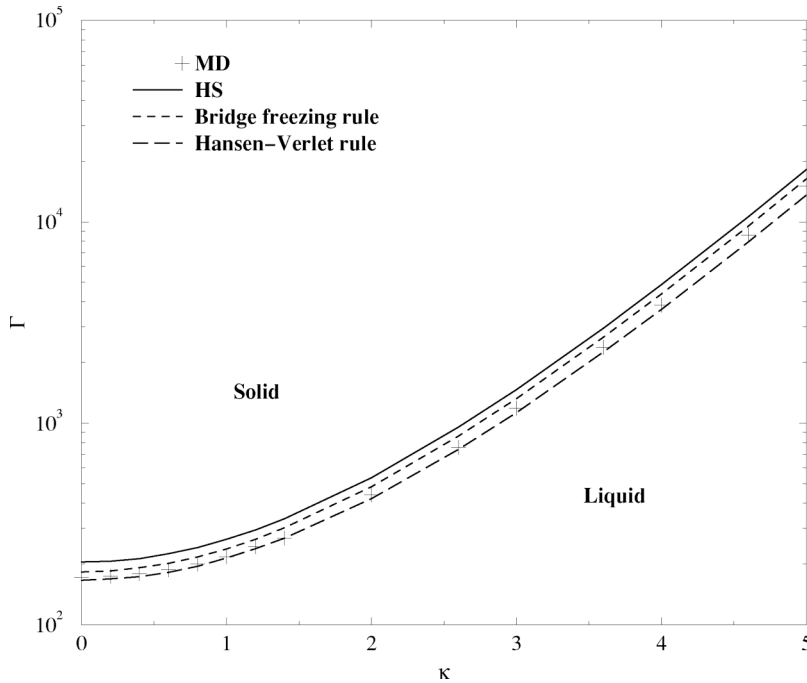


FIG. 1. Phase diagram of the Yukawa system in the  $\{\Gamma, \kappa\}$  plane. The liquid-solid phase boundary is shown as predicted by the molecular dynamics results of Hamaguchi *et al.* [13] (MD) and by the VMHNC theory using the effective HS closed-packing fraction at melting (VMHNC<sup>a</sup> or HS) [14], the semiempirical freezing criteria using the Bridge function (VMHNC<sup>b</sup> or Bridge freezing rule) [70], and the structure factor (VMHNC<sup>c</sup> or the Hansen-Verlet rule) [71].

cient for our business. But the minimum value of the functional  $\mathcal{F}(c_n, \eta)$  depends on  $\alpha_{HOF}$  and  $N_{HOF}$  too. We have tested on some examples that at fixed number of HOF, there exists an optimal value for  $\alpha_{HOF}$ , which gives the best minimum for  $\mathcal{F}(c_n, \eta)$ . Moreover, the larger is  $N_{HOF}$ , the flatter is the curve around the minimum. This means that when  $N_{HOF}$  is large, the expansion of  $c_S(r)$  upon the HOF does not depend very much on  $\alpha_{HOF}$  around the minimum due to the complete character of the basis. Yet, we have not implemented a refined algorithm to optimize  $\alpha_{HOF}$  and  $N_{HOF}$  for the reasons explained above. Again, all these comments extend straightforwardly to the VMHNC excess free energy that could be considered as an algebraic function of  $\beta$ ,  $\rho_i$ ,  $\eta$ ,  $\{c_n\}$ ,  $N_{HOF}$ , and  $\alpha_{HOF}$ . Moreover, powerful conjugate-gradient algorithms [65,64] could be of great interest to achieve its minimization with respect to  $\eta$  and  $\{c_n\}$ . Finally, this general approach of expanding  $c_S(r)$  in the 3D spherical HOF can be generalized to treat mixture [50] and nonspherical potential [60]. This paper suggests the existence of an interesting gap between nuclear physics, condensed matter, and plasma physics. Works are in progress in this field.

### III. THERMODYNAMIC PROPERTIES

The VMHNC theory predictions concerning the thermodynamics of the Yukawa system are compared to the extensive molecular dynamics simulation results by Hamaguchi *et al.* [11–13]. The liquid-solid phase boundary, thermodynamic consistency, and equation of state are discussed. The regimes of weak screening and strong screening for Yukawa fluid are considered.

#### A. Phase diagram

To quantify the accuracy of the VMHNC theory, the liquid-solid phase boundary of the Yukawa fluid is predicted

and compared to the simulation data of Hamaguchi *et al.* [13]. The phase boundary is first found by solving for the critical HS parameter  $\eta_c$  and for various  $\kappa$  the equation

$$\eta_c = \eta_{eff}(\Gamma, \kappa), \quad (24)$$

where  $\Gamma$  is the unknown. The critical  $\eta_c$ , at which the HS system is known to solidify, is equal to  $\eta_c = 2\eta_{cp}/3$ .  $\eta_{cp}$  is the closed-packing fraction  $\eta_{cp} = \pi/3/\sqrt{2}$  [68]. This procedure (VMHNC<sup>a</sup>) is identical to the one proposed in Ref. [14]. Results are plotted in Fig. 1. Following Rosenfeld [69], we have added two more indicators to detect the critical  $\Gamma_c$  at which the YOCP fluid begins to freeze. We have used the “Bridge freezing rule” (VMHNC<sup>b</sup>), stressing that the Bridge function absolute value at the origin  $B_0 = |B(0, \Gamma, \kappa)|$  is nearly equal to 50 [70], and the “Hansen-Verlet rule” (VMHNC<sup>c</sup>), i.e.,  $S(k)_{Max} \approx 3$  at freezing [71]. We have thus solved for various  $\kappa$  the equations

$$|B(0, \Gamma, \kappa)| = 50 \quad (25)$$

and

$$S(k)_{Max}(\Gamma, \kappa) = 3, \quad (26)$$

where  $\Gamma$  is the unknown. The agreement with the simulation data is excellent considering the simplicity of the theory. Indeed, it was not clear *a priori* which physical meaning could be attributed to the effective HS packing fraction of the VMHNC. It is also a nice confirmation of the Bridge freezing rule. However, we should confess that the Hansen-Verlet rule is the most robust way to detect freezing. To be complete, we give the associated maximum value of the structure factor  $S(k)_{Max}$ , minus the excess entropy  $-s_Y^{ex}$  (see below), and the absolute value of the Bridge function at the origin  $B_0 =$  for the exact values of  $\Gamma_c$  determined by Hamaguchi *et al.* [13] in Table I. Again, we confirm the pertinence of the

TABLE I. Maximum values of structure factor  $S(k)_{Max}$ , minus excess entropy  $-s_Y^{ex}$ , and absolute value of the Bridge function at the origin  $B_0$  calculated using the VMHNC theory at the fluid-solid phase-transition values  $\Gamma_c$  deduced from MD simulations by Hamaguchi *et al.* [13].

$\kappa$	MD	$S(k)_{Max}$	$-s_Y^{ex}$	$B_0$
0.0	171.8	3.058	4.152	47.12
0.2	173.5	3.058	4.144	47.08
0.4	178.6	3.054	4.123	46.93
0.6	187.1	3.045	4.091	46.64
0.8	199.6	3.035	4.052	46.25
1.0	217.4	3.026	4.016	45.93
1.2	243.3	3.035	3.997	45.99
1.4	268.8	3.000	3.925	44.76
2.0	440.1	3.070	3.921	45.71
2.6	758.9	3.042	3.835	44.23
3.0	1185.	3.081	3.855	44.88
3.6	2378.	3.089	3.849	44.75
4.0	3837.	3.068	3.825	44.06
4.6	8609.	3.124	3.899	45.52
5.0	15060.	3.161	3.954	46.57

Hansen-Verlet rule and the reasonable agreement with the Bridge freezing rule and the semiempirical rule of Rosenfeld [72], which states that excess entropy, i.e., the reduced configurational entropy, is close to 4 at freezing.

### B. Thermodynamic consistency

The existence of a free energy  $F$  within the VMHNC theory guarantees that internal energy  $U=F-T\partial F/\partial T|_{\Omega}$  and pressure  $P=-\partial F/\partial\Omega|_T$  satisfy the fundamental equation

$$\left.\frac{\partial U}{\partial\Omega}\right|_T = T \left.\frac{\partial P}{\partial T}\right|_{\Omega} - P, \quad (27)$$

where

$$\frac{\beta U}{N} = \frac{3}{2} + \frac{\rho_i}{2} \int \beta \phi(r) g(r) d\mathbf{r}, \quad (28)$$

$$\frac{P}{P_0} = 1 - \frac{\rho_i}{6} \int \beta r \phi'(r) g(r) d\mathbf{r},$$

and  $P_0 = \rho_i/\beta$ . The VMHNC theory ensures thus the thermodynamic consistency between the Helmholtz free energy and the virial routes to the equation of state, and the energy  $U$  and the virial pressure  $P$  equations of state pass the Hiroike's test [52]. This is clearly true for Yukawa system, as long as the effective inverse screening length is independent of temperature and density. This is the case here, replacing, as usual,  $\phi(r)$  and  $g(r)$  by  $v_Y(r)$  and  $h(r)$ , respectively, and adding the energy reference term  $\beta\mathcal{E}$ . However, great care is required for state-dependent potential  $\phi(r, T, \rho_i)$  [73–75]. In such a situation, the dependency of the pair potential with respect to  $T$  and  $\rho_i$  brings additional terms in the calculation

of pressure and internal energy by quadrature. The standard quadrature formulas lose meaning and interest, especially when the behavior of  $\phi(r, T, \rho_i)$  with respect to  $T$  and  $\rho_i$  is complicated and sometimes even unknown analytically. Such a situation is typically encountered in liquid metal theory or dense plasma physics. This explains why the thermodynamic consistency between the compressibility and the virial routes is not enforced in the VMHNC, though known to be reasonably good [48,49]. This means that the partial differentiation of pressure with respect to density at constant temperature should satisfy

$$\beta \left.\frac{\partial P}{\partial\rho_i}\right|_T = 1 - \rho_i \int c(r) d\mathbf{r} \quad (29)$$

for general pairwise, state-independent, and with no background potential  $\phi(r)$ . For YOCP, this relation reads

$$\beta \left.\frac{\partial P}{\partial\rho_i}\right|_T = 1 - \rho_i \int [c(r) + \beta v_Y(r)] d\mathbf{r}. \quad (30)$$

When one faces state-dependent potential, there is no way but differentiating analytically in the best case, numerically in the worse case, the free energy of the system. This can always be done in the framework of the VMHNC, but rules out any other theory that does not stand, from the beginning, on a free energy (even effective or approximate). One can realize why enforcing the thermodynamic consistency between the compressibility and the virial routes appears to be not so crucial in the VMHNC theory.

A wide range of physical conditions may be described by simple relations if we choose the dimensionless quantities  $\Gamma$  and  $\kappa$ , in lieu of the particle density  $\rho_i$  and temperature  $T$  (or inverse temperature  $\beta$ ), as independent thermodynamic variables. Since the effective inverse screening length of the considered Yukawa system is constant, the transformation of standard thermodynamic equations to dimensionless form is then governed by the relations

$$\rho_i \left.\frac{\partial\Gamma}{\partial\rho_i}\right|_{\beta} = \frac{\Gamma}{3} \quad \text{and} \quad \beta \left.\frac{\partial\Gamma}{\partial\beta}\right|_{\rho_i} = \Gamma, \quad (31)$$

$$\rho_i \left.\frac{\partial\kappa}{\partial\rho_i}\right|_{\beta} = -\frac{\kappa}{3} \quad \text{and} \quad \beta \left.\frac{\partial\kappa}{\partial\beta}\right|_{\rho_i} = 0. \quad (32)$$

Given the free energy  $F=U-TS$  of the system in function of  $T$  and  $\rho_i$ , where entropy  $S=-\partial F/\partial T|_{\Omega}$ , the relations defining  $U$ ,  $P$ , and  $S$  can be recast in terms of dimensionless intensive variables [11,14]

$$u = \beta \left.\frac{\partial f}{\partial\beta}\right|_{\rho_i}, \quad p = \rho_i \left.\frac{\partial f}{\partial\rho_i}\right|_{\beta}, \quad \text{and} \quad s = u - f, \quad (33)$$

where

$$f = \frac{\beta F}{N}, \quad u = \frac{\beta U}{N}, \quad p = \frac{\beta P}{\rho_i}, \quad \text{and } s = \frac{S}{Nk_B}. \quad (34)$$

$f$ ,  $u$ ,  $p$ , and  $s$  denote the free and internal energies per particle in units of  $k_B T$ , the pressure in units of  $\rho_i k_B T$ , and the entropy per particle in units of  $k_B$ .

Once known the free energy as a function of  $f(\Gamma, \kappa)$  of the parameters  $\Gamma$  and  $\kappa$ , internal energy, pressure, and entropy can be determined as functions of these variables using Eq. (31) and the chain rule to rewrite Eq. (33),

$$u = \Gamma \frac{\partial f}{\partial \Gamma}, \quad p = -\frac{\kappa}{3} \frac{\partial f}{\partial \kappa} + \frac{\Gamma}{3} \frac{\partial f}{\partial \Gamma}, \quad \text{and } s = u - f. \quad (35)$$

The ideal-gas behavior is recovered in the limit  $\Gamma \rightarrow 0$ . In that limit [14,23]

$$\begin{aligned} f &\rightarrow f^0 = \ln(\rho_i) + \frac{3}{2} \ln(\beta) + \frac{3}{2} \ln\left(\frac{2\pi \hbar^2}{m}\right) - 1, \\ u &\rightarrow u^0 = \frac{3}{2}, \\ p &\rightarrow p^0 = 1, \\ s &\rightarrow s^0 = u^0 - f^0. \end{aligned} \quad (36)$$

The deviation with respect to the ideal components  $f^0$ ,  $u^0$ ,  $s^0$ , and  $p^0$  comes from interactions between particles and constitutes obviously the nontrivial part of the problem. Subtracting the ideal-gas contribution  $f^0$ ,  $u^0$ ,  $s^0$ , and  $p^0$  from  $f$ ,  $u$ ,  $s$ , and  $p$ , respectively, allows us to define the excess free energy  $f^{ex}$ , the excess internal energy  $u^{ex}$ , the excess entropy  $s^{ex}$ , and the excess pressure  $p^{ex}$ . For Yukawa system practical formulas of interest read finally in units of  $a_{WS}$ ,

$$\begin{aligned} u_Y^{ex}(\Gamma, \kappa) &= \frac{3}{8\pi} \int u_Y(r) h(r) d\mathbf{r} - \frac{\Gamma \kappa}{2}, \\ f_Y^{ex}(\Gamma, \kappa) &= \int_0^\Gamma \frac{u_Y^{ex}(\Gamma', \kappa)}{\Gamma'} d\Gamma', \\ s_Y^{ex}(\Gamma, \kappa) &= u_Y^{ex} - f_Y^{ex}, \\ p_Y^{ex}(\Gamma, \kappa) &= -\frac{1}{8\pi} \int r u_Y'(r) h(r) d\mathbf{r}. \end{aligned} \quad (37)$$

The function  $(\Gamma, \kappa) \rightarrow p_Y^{ex}(\Gamma, \kappa)$  is the equation of state for the Yukawa system. An accurate representation of this function is of practical interest in, for instance, the formulation of macroscopic descriptions for the behavior of dust/plasma suspensions that can help in understanding and controlling particulate contamination in industrial process plasmas. Note also that this function is not universal for given  $(\Gamma, \kappa)$ . Indeed, the effective screening length, assumed constant here, may depend on temperature  $T$  and particle density  $\rho_i$  [11]. This fact is hidden in the variable change formulas (31) between  $(\rho_i, T)$  space and  $(\Gamma, \kappa)$  space. So, erroneous conclu-

sions may be drawn from a blind one-to-one correspondence between formalism and practical applications. Finally, when the VMHNC is employed, i.e.,

$$f_Y^{ex}(\Gamma, \kappa) = f_Y^{VMHNC}(\Gamma, \kappa, \eta), \quad (38)$$

the thermodynamic quantities of interest should be read  $f_Y^{ex, VMHNC}$ ,  $u_Y^{ex, VMHNC}$ ,  $s_Y^{ex, VMHNC}$ , and  $p_Y^{ex, VMHNC}$ .

As an illustration, we have checked the VMHNC thermodynamic consistency between the compressibility and the virial routes for YOCP for integer  $\kappa \in [0, 5]$ . Equation (27) reduces to

$$\rho_i \left. \frac{\partial u}{\partial \rho_i} \right|_\beta = \beta \left. \frac{\partial p}{\partial \beta} \right|_{\rho_i} \quad (39)$$

or

$$\frac{\Gamma}{3} \left. \frac{\partial u_Y^{ex}}{\partial \Gamma} \right|_\kappa - \frac{\kappa}{3} \left. \frac{\partial u_Y^{ex}}{\partial \kappa} \right|_\Gamma = \Gamma \left. \frac{\partial p_Y^{ex}}{\partial \Gamma} \right|_\kappa, \quad (40)$$

whereas the virial-compressibility consistency reads

$$\begin{aligned} p_Y^{ex} + 1 + \frac{\Gamma}{3} \left. \frac{\partial p_Y^{ex}}{\partial \Gamma} \right|_\kappa - \frac{\kappa}{3} \left. \frac{\partial p_Y^{ex}}{\partial \kappa} \right|_\Gamma \\ = 1 - \frac{3}{4\pi} \int [c_{Y,S}(r) + u_{Y,S}(r)] d\mathbf{r} \end{aligned} \quad (41)$$

in  $a_{WS}$  units. Let us introduce the normalized temperature  $T^*$  as the ratio of the system temperature  $T$  to the fluid-solid melting temperature or critical temperature  $T_c$ , i.e.,  $T^* = T/T_c = \Gamma_c/\Gamma$ . The normalized temperature has been shown to be very convenient to describe Yukawa system and to find general trends or universal behaviors [13,19,20]. We have plotted in Fig. 2 the excess compressibility normalized to the coupling parameter  $\Gamma$  in function of inverse normalized temperature  $t^* = 1/T^*$ , obtained by quadrature using the compressibility equation (30),

$$t^* \rightarrow -\frac{3}{4\pi\Gamma} \int [c_{Y,S}(r) + u_{Y,S}(r)] d\mathbf{r}, \quad (42)$$

and the numerical differentiation of  $\beta \partial P / \partial \rho_i|_\beta$  calculated from the virial equation (28),

$$t^* \rightarrow \frac{p_Y^{ex}}{\Gamma} + \frac{1}{3} \left. \frac{\partial p_Y^{ex}}{\partial \Gamma} \right|_\kappa - \frac{\kappa}{3\Gamma} \left. \frac{\partial p_Y^{ex}}{\partial \kappa} \right|_\Gamma. \quad (43)$$

The partial differentiations are performed using Chebyshev polynomials [64]. A variation of 0.1 % is made for  $\Gamma$  and  $\kappa$  around the reference point  $(\Gamma, \kappa)$  and eight polynomials are sufficient to calculate the partial derivatives with good accuracy. We find that the virial-compressibility inconsistency is rather small (less than 20% for OCP which is the worst case) over the entire Yukawa fluid plan for the screening parameters considered. This fact is remarkable since the thermodynamic consistency between virial and compressibility routes is not enforced *a priori* in the VMHNC theory.

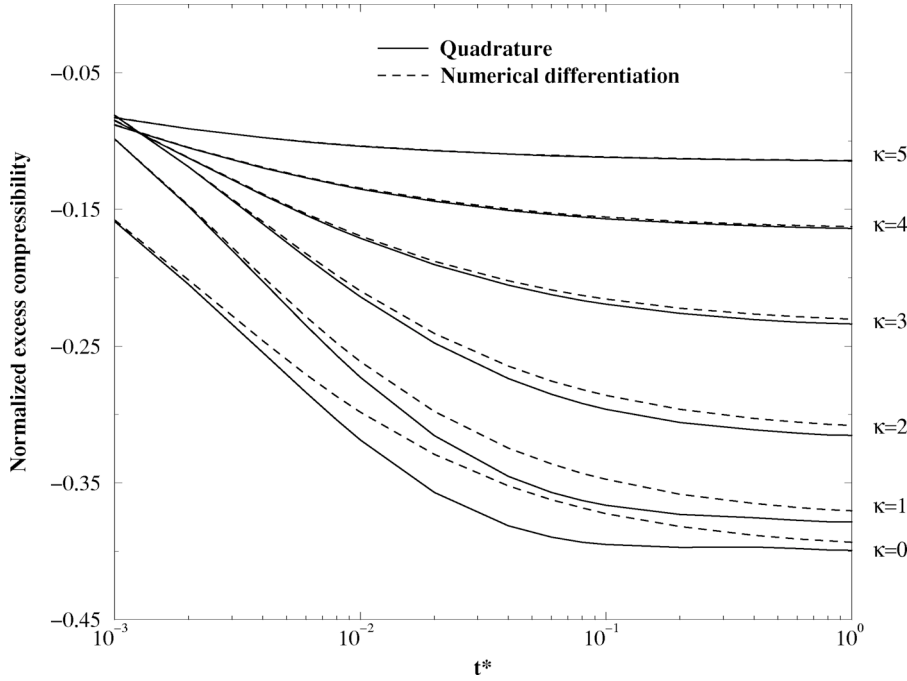


FIG. 2. Excess compressibility normalized to coupling parameter  $\Gamma$  vs inverse normalized temperature  $t^*$ . Quadrature (solid line) means that the normalized excess compressibility is computed directly from the compressibility equation (42). Numerical differentiation (dashed line) means that the normalized excess compressibility is computed differentiating the pressure or virial eq. (43).

### C. Excess internal energy

For strong coupling ( $\Gamma > 1$ ), Hamaguchi *et al.* gave two fitting formulas for  $u_Y^{ex}$  for the cases of weak screening ( $\kappa \leq 1$ ) [11,12] and strong screening ( $\kappa \geq 1$ ) [13], respectively. In the weak-screening case, Hamaguchi *et al.* [11,12] proposed to fit their molecular dynamics data by the formula

$$u_{Y,MD}^{ex}(\Gamma, \kappa) = a(\kappa)\Gamma + b(\kappa)\Gamma^s + c(\kappa) + d(\kappa)\Gamma^{-s}, \quad (44)$$

with  $s=1/3$ . Using the Magdelug energy for bcc Yukawa lattices,

$$E_{bcc}(\kappa) = -0.895\,929 - 0.103\,731\kappa^2 + 0.003\,084\kappa^4 - 0.000\,131\kappa^6, \quad (45)$$

$$a(\kappa) = E_{bcc}(\kappa) + \delta a(\kappa), \quad (46)$$

and

$$\delta a(\kappa) = -0.003\,366 + 0.000\,660\kappa^2 - 0.000\,089\kappa^4,$$

$$b(\kappa) = 0.565\,004 - 0.026\,134\kappa^2 - 0.002\,689\kappa^4,$$

$$c(\kappa) = -0.206\,893 - 0.086\,384\kappa^2 - 0.018\,278\kappa^4,$$

$$d(\kappa) = -0.031\,402 + 0.042\,429\kappa^2 - 0.008\,037\kappa^4. \quad (47)$$

In the strong-screening case, Hamaguchi *et al.* [12,13] do not use Taylor expansion in  $\kappa$  for the coefficients, as defined by Eqs. (45)–(47). Instead, they fit the potential energy functional forms of Eq. (44) directly to the simulation data for each  $\kappa$  value separately. Data can be found for some values of  $\kappa$  in Table VIII of Ref. [13].

For weak coupling ( $\Gamma \leq 1$ ), Eq. (44) is no longer valid. We have thus decided to use the values of  $u_{Y,MD}^{ex}(\Gamma, \kappa)/\Gamma$  given in Table IV, p. 9889 of Ref. [11] and Table VI of Ref.

[13] to expand it in Chebyshev polynomials using spline technique [64] for  $\Gamma \in [0, 1]$  at fixed  $\kappa$ .  $u_{Y,MD}^{ex}(\Gamma, \kappa)$  is then known for any value of  $\Gamma \in [0, 1]$ .

We have plotted in Fig. 3 excess internal energy normalized to  $\Gamma$  versus inverse normalized temperature  $t^*$  using VMHNC theory, i.e.,  $u_{Y,VMHNC}^{ex}/\Gamma$  and MD results, i.e.,  $u_{Y,MD}^{ex}/\Gamma$  for integer  $\kappa \in [0, 5]$ . Agreement between MD and VMHNC results is excellent.

### D. Excess free energy

$f_Y^{ex}$  can be obtained from  $u_Y^{ex}$  by quadrature using Eq. (35). For strong coupling, the excess free energy can be integrated analytically with the result

$$f_{Y,MD}^{ex}(\Gamma, \kappa) = \int_1^\Gamma u_{Y,MD}^{ex}(\Gamma', \kappa) \frac{d\Gamma'}{\Gamma'} + f_1(\kappa) = a(\kappa)(\Gamma - 1) + b(\kappa) \frac{\Gamma^s - 1}{s} + c(\kappa) \ln(\Gamma) - d(\kappa) \frac{\Gamma^{-s} - 1}{s} + f_1(\kappa) \quad (48)$$

with

$$f_1(\kappa) = \int_0^1 u_{Y,MD}^{ex}(\Gamma', \kappa) \frac{d\Gamma'}{\Gamma'}. \quad (49)$$

No fit was proposed for  $f_1(\kappa)$  calculated through a direct Simpson-rule quadrature of the  $u_{Y,MD}^{ex}/\Gamma$  values obtained from molecular dynamics simulations. Data can be found for some values of  $\kappa$  in Table VII of Ref. [13]. For weak coupling,  $f_{Y,MD}^{ex}(\Gamma, \kappa)$  is integrated numerically using Chebyshev polynomial properties [64]. Excess free energy is thus available for any value of  $\Gamma \in [0, 1]$ . We have plotted in Fig. 4 excess free energy normalized to  $\Gamma$  versus inverse normalized temperature  $t^*$  using VMHNC theory, i.e.,  $f_{Y,VMHNC}^{ex}/\Gamma$

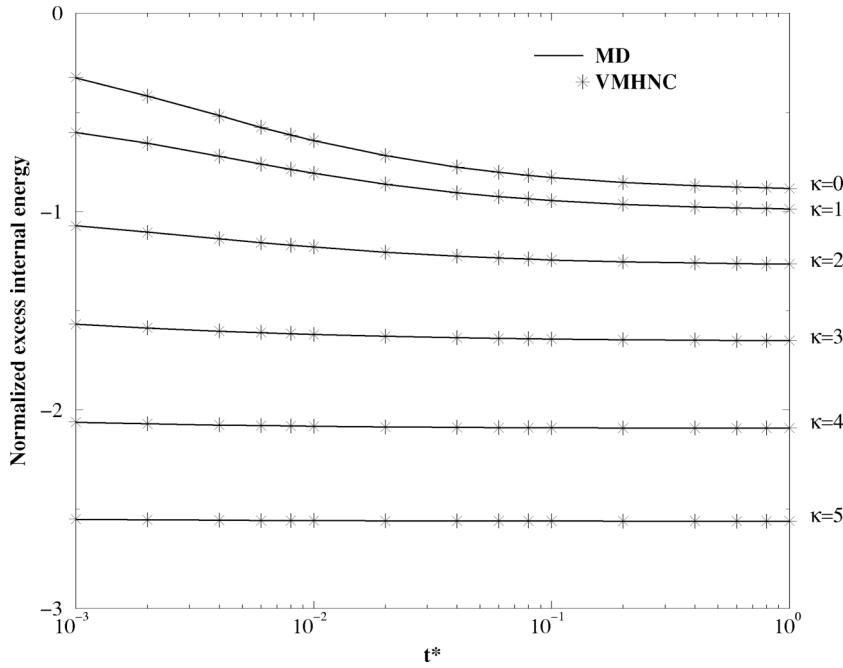


FIG. 3. Excess internal energy normalized to coupling parameter  $\Gamma$  vs inverse normalized temperature  $t^*$  as predicted by the VMHNC theory (asterisk) and the simulation results (solid line) for the Yukawa system using the procedure and the fits proposed by Hamaguchi *et al.* [11–13] for integer  $\kappa \in [0, 5]$ .

and MD results, i.e.,  $f_{Y,MD}^{ex}/\Gamma$  for integer  $\kappa \in [0, 5]$ . As for excess internal energy, agreement between the VMHNC theory predictions and simulation results is excellent.

### E. Excess entropy

Once excess internal energy  $u_{Y,MD}^{ex}$  and excess free energy  $f_{Y,MD}^{ex}$  are known, excess entropy  $s_{Y,MD}^{ex}$  can easily be obtained from the relation  $s_{Y,MD}^{ex} = u_{Y,MD}^{ex} - f_{Y,MD}^{ex}$  using Eq. (35). We have plotted in Fig. 5 minus excess entropy versus inverse normalized temperature  $t^*$  using VMHNC theory, i.e.,  $-s_{Y,VMHNC}^{ex}$  and MD results, i.e.,  $-s_{Y,MD}^{ex}$  for integer  $\kappa$

$\in [0, 5]$ . As above, VMHNC theory predictions agree very well with simulation results. Moreover, one sees that minus excess entropy tends towards 4 when  $t^* \rightarrow 1$ , i.e., in the vicinity of the liquid-solid phase boundary.

### F. Excess pressure

As for excess pressure  $p_{Y,MD}^{ex}$  we can use Eq. (35) and recover Eq. (27) of Ref. [11] changing  $\kappa/6$  by  $-\kappa/3$ , due to the different particle density and temperature of our model and the one studied by Hamaguchi *et al.* [11]. For strong coupling, we find

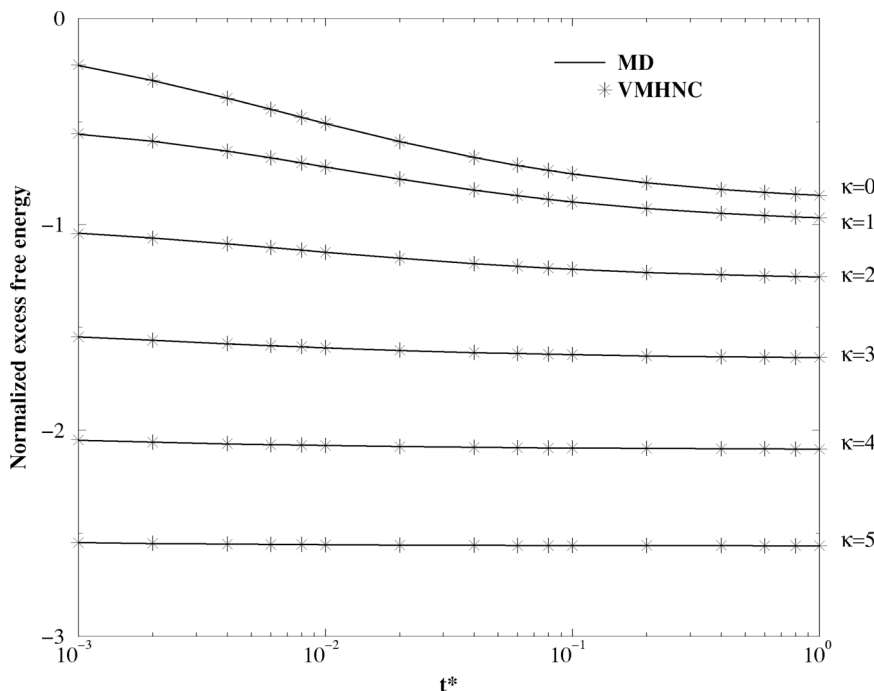


FIG. 4. Excess free energy normalized to coupling parameter  $\Gamma$  vs inverse normalized temperature  $t^*$  as predicted by the VMHNC theory (star) and the simulation results (solid line) for the Yukawa system using the procedure and the fits proposed by Hamaguchi *et al.* [11–13] for integer  $\kappa \in [0, 5]$ .

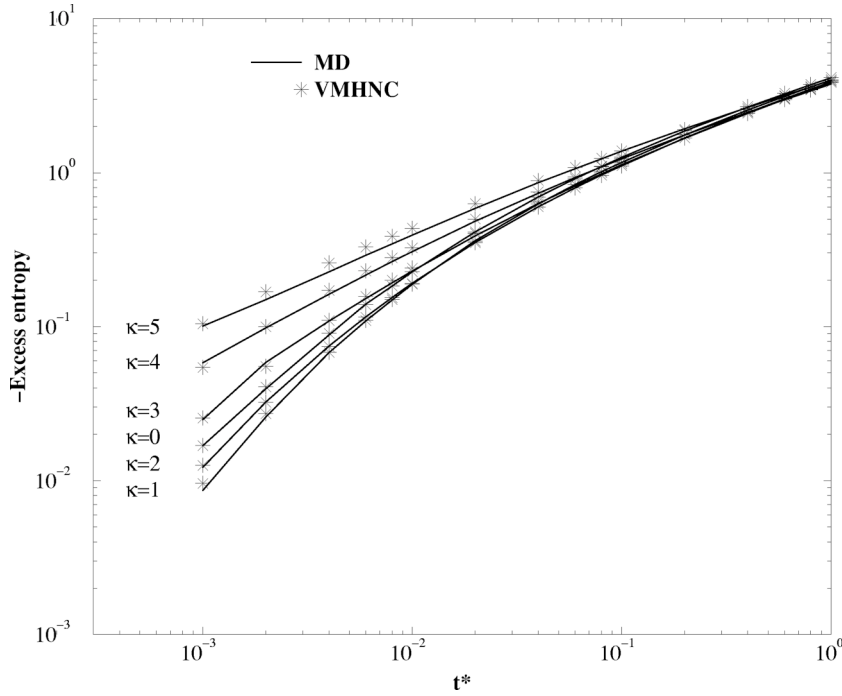


FIG. 5. Minus excess entropy vs inverse normalized temperature  $t^*$  as predicted by the VMHNC theory (asterisk) and the simulation results (solid line) for the Yukawa system using the procedure and the fits proposed by Hamaguchi *et al.* [11–13] for integer  $\kappa \in [0, 5]$ .

$$p_{Y,MD}^{ex}(\Gamma, \kappa) = \frac{1}{3} \left[ a(\kappa)\Gamma + b(\kappa)\Gamma^s + c(\kappa) + d(\kappa)\Gamma^{-s} \right],$$

$$- \frac{\kappa}{3} \left[ \frac{da(\kappa)}{d\kappa} (\Gamma - 1) + \frac{db(\kappa)}{d\kappa} \frac{\Gamma^s - 1}{s} \right.$$

$$\left. + \frac{dc(\kappa)}{d\kappa} \ln(\Gamma) - \frac{dd(\kappa)}{d\kappa} \frac{\Gamma^{-s} - 1}{s} + \frac{df_1(\kappa)}{d\kappa} \right]. \quad (50)$$

Functions  $da(\kappa)/d\kappa$ ,  $db(\kappa)/d\kappa$ ,  $dc(\kappa)/d\kappa$ , and  $dd(\kappa)/d\kappa$  are known analytically for  $\kappa \in [0, 1]$  only. For stronger screening, one has kept the strategy encountered above for calcu-

lating excess internal energy for  $\Gamma \leq 1$ . We have used the values of Table VIII of Ref. [13] to expand  $a(\kappa)$ ,  $b(\kappa)$ ,  $c(\kappa)$ , and  $d(\kappa)$  in Chebyshev polynomials using spline technique [64] for  $\kappa \in [1, 5]$ . Each function and its derivative are then known for  $\kappa \in [1, 5]$ . For weak coupling, excess pressure is obtained by numerical differentiation of excess free energy using again known properties of Chebyshev polynomials [64]. We have plotted in Fig. 6 excess pressure normalized to  $\Gamma$  versus inverse normalized temperature  $t^*$  using VMHNC theory, i.e.,  $p_{Y,VMHNC}^{ex}$  and MD results, i.e.,  $p_{Y,MD}^{ex}$  for integer  $\kappa \in [0, 5]$ . Good agreement is still found between VMHNC theory predictions and simulation results.

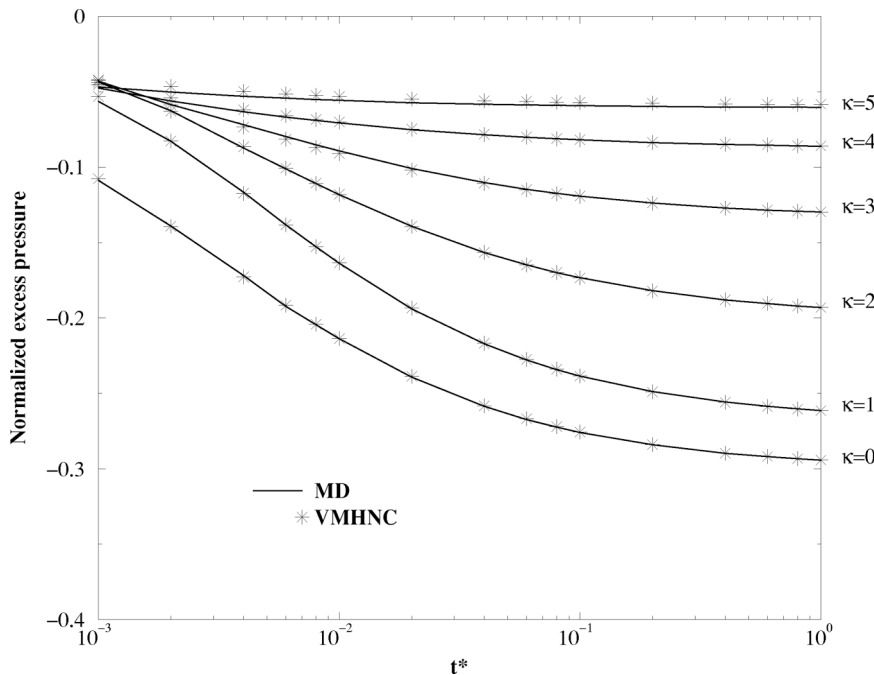


FIG. 6. Excess pressure normalized to coupling parameter  $\Gamma$  as predicted by the VMHNC theory (asterisk) and the simulation results (solid line) for the Yukawa system using the procedure and the fits proposed by Hamaguchi *et al.* [11–13] for integer  $\kappa \in [0, 5]$ .

#### IV. TRANSPORT COEFFICIENTS

Transport coefficients such as self-diffusion, viscosity, and thermal conductivity are the most fundamental dynamical parameters that reflect the nature of the interparticle potentials and characterize the thermodynamics of the system. The VMHNC approach is used in order to estimate the self-diffusion, the shear viscosity, and the thermal conductivity of the Yukawa system from the transport coefficients of the HS system. Comparisons with MD data are done in a systematic manner over a wide range of the system parameters  $\{\Gamma, \kappa\}$ . Our goal is to see whether it is possible to predict dynamic properties of Yukawa systems from the VMHNC theory that is only valid for studying static properties of systems in thermodynamical equilibrium.

##### A. Diffusion

The self-diffusion coefficient will be denoted by  $D$ . Many conventions exist for normalizing the diffusion coefficient that display quasiuniversal characteristics. Some of these are by Hansen *et al.* [76]  $D' = D/D_{pf}$ , by Ohta and Hamaguchi [19]  $D^* = D/D_{ef}$ , and by Rosenfeld [17,18,72,77]  $D^r = D/D_{md}$ , where  $D_{pf} = \omega_p a_{WS}^2$ ,  $D_{ef} = \omega_e a_{WS}^2$ , and  $D_{md} = \rho_i^{-1/3} \sqrt{k_B T/m}$ . Here,  $D_{md}$ ,  $\omega_e$ , and  $\omega_p = \sqrt{4\pi\rho_i Q^2/m}$  are the macroscopic diffusion, the Einstein frequency, and the plasma frequency, respectively. The ratio between the plasma frequency and the Einstein frequency can be obtained from a fit to the result of Ohta and Hamaguchi [19] as

$$\frac{\sqrt{3}\omega_e}{\omega_p} = e^{-0.2058\kappa^{1.590}}. \quad (51)$$

Note that the Einstein frequency accounts for variations in the vibration frequency due to screening.

Pioneer work has been done by Hansen *et al.* [76] for the OCP system using MD simulations. They were able to propose an efficient fit for the OCP diffusion coefficient that was shown to obey a power law with respect to  $\Gamma$ . This law is valid for strong coupling but fails when  $\Gamma$  is around one or below. More recently, Ohta and Hamaguchi [19] found that the self-diffusion coefficients in Yukawa systems follow a simple scaling law with respect to normalized temperature  $T^*$ . They fit their MD data to the form

$$D^* = \alpha_\kappa (T^* - 1)^{\beta_\kappa} + \gamma_\kappa \quad (52)$$

for each  $\kappa$ . They were also able to fit the OCP simulation data by Hansen *et al.* [76] to this same and more accurate form, compared to the original power law.

As for HS system, the Enskog's theory for hard sphere is remarkably accurate when compared to simulations [18]. We propose to use a fit to the relatively small corrections to Enskog, as obtained from the most recent simulations for the hard-sphere fluid [78]. Normalizing in terms of  $D_{ef}$ , the Yukawa diffusion may be obtained from the HS result  $D_{HS}$  as

$$D_{YHS}^*(\Gamma, \kappa) \equiv \frac{D_{HS}}{D_{ef}} = \frac{D_{HS}}{D_E} \frac{D_E}{D_{gas}} \frac{D_{gas}}{D_{ef}}, \quad (53)$$

where

$$\frac{D_{HS}}{D_E} = 1.01896(1 + 0.073\eta + 11.6095\eta^2 - 26.951\eta^3),$$

$$\frac{D_E}{D_{gas}} = \frac{(1-\eta)^3}{(1-\eta/2)},$$

$$\frac{D_{gas}}{D_{ef}} = \frac{1}{8\eta^{2/3}} \sqrt{\frac{\pi}{\Gamma}} e^{0.2058\kappa^{1.590}}. \quad (54)$$

Here,  $D_{gas}$  and  $D_E$  are the results for a dilute gas and the Enskog's result, respectively. Note that the CS equation of state for the radial pair distribution function at contact has been used [14]. In Eq. (53),  $\eta$  is the effective hard-sphere packing fraction of the Yukawa system determined by the VMHNC method. In Eq. (53), Y refers to Yukawa and HS to hard sphere.

##### B. Viscosity

The shear viscosity will be denoted by  $\eta_v$  to distinguish it from the HS packing fraction  $\eta$ . The definitions of normalized shear viscosities are given by  $\eta' = \eta_v/\eta_{pf}$  [23],  $\eta^* = \eta_v/\eta_{ef}$  [20], and  $\eta^r = \eta_v/\eta_{mv}$  [17,18,72,77], where  $\eta_{pf} = m\rho_i\omega_p a_{WS}^2$ ,  $\eta_{ef} = m\rho_i\sqrt{3}\omega_e a_{WS}^2$ , and  $\eta_{mv} = \rho_i^{2/3}\sqrt{mk_B T}$ . Here,  $\eta_{mv}$  is the macroscopic viscosity. Note that  $\eta^* = \eta'$  when  $\kappa = 0$ , i.e., for OCP system. The normalization employed for  $\eta'$  has been widely used for the OCP system [23]. The normalization used for  $\eta^*$  has been shown to be more suited for Yukawa systems and is considered to be a natural extension of  $\eta'$  of the OCP in finite screening (i.e.,  $\kappa \neq 0$ ) [20].

Using kinetic theory, Wallenborn and Baus [79] found an approximate analytical formula for the OCP shear viscosity. More recently, Saigo and Hamaguchi [20] proposed a different analytical formula to fit their MD calculations of shear viscosity for Yukawa system that can be used for OCP system as well.  $\eta^*$  can be simply represented for each  $\kappa$  by

$$\eta^* = a_\kappa T^* + \frac{b_\kappa}{T^*} + c_\kappa, \quad (55)$$

where  $T^*$  is the normalized temperature defined above. This formula applied to the OCP system was found [14] to be more accurate than the former one proposed by Wallenborn and Baus [79].

As for HS system, the Enskog's theory for hard sphere is remarkably accurate when compared to simulations, i.e., for  $\eta < \eta_{cp}/5$  [18], except near the liquid-solid phase boundary of the HS system, where the discrepancy may reach a factor 2 [23,80]. Furthermore, the Stokes relation with slip conditions, i.e.,  $D\eta_v = k_B T/(2\pi\sigma)$ , has been found to be remarkably precise (i.e., for  $\eta > \eta_{cp}/5$ ) [80]. Unfortunately, we neither have more recent MD calculations nor any analytical expression for the HS shear viscosity. As a consequence, since we know the self-diffusion coefficient for HS system with high precision [18,78], one solution would be to estimate HS viscosity using the Stokes relation for  $\eta > \eta_{cp}/5$  and simply the Enskog's result for  $\eta < \eta_{cp}/5$ , i.e., in the gas phase. However, in order to avoid discontinuity or treat the delicate joining question by a smooth interpolation between

both domains, we propose to use a fit [14] to the corrections to Enskog, as obtained from the simulations for the hard-sphere fluid [80]. The Yukawa diffusion may thus be obtained from the HS result as

$$\eta_{YHS}^*(\Gamma, \kappa) \equiv \frac{\eta_{HS}}{\eta_{ef}} = \frac{\eta_{HS}}{\eta_E} \frac{\eta_E}{\eta_{gas}} \frac{\eta_{gas}}{\eta_{ef}}, \quad (56)$$

where

$$\begin{aligned} \frac{\eta_{HS}}{\eta_E} &= (1 + 2.5502\eta - 23.0982\eta^2 + 44.1238\eta^3), \\ \frac{\eta_E}{\eta_{gas}} &= \left[ \frac{(1-\eta)^3}{(1-\eta/2)} + 0.800(4\eta) + 0.761(4\eta)^2 \frac{(1-\eta/2)}{(1-\eta)^3} \right], \\ \frac{\eta_{gas}}{\eta_{ef}} &= \frac{5}{48\sqrt{3}\eta^{2/3}} \sqrt{\frac{\pi}{\Gamma}} e^{0.2058\kappa^{1.590}}. \end{aligned} \quad (57)$$

Here,  $\eta_{gas}$  and  $\eta_E$  are the result for a dilute gas and the Enskog's result, respectively. Note that the CS equation of state for the radial pair distribution function at contact has been used [14]. In Eq. (56),  $\eta$  is the effective hard-sphere packing fraction of the Yukawa system determined by the VMHNC method. In Eq. (56), Y refers to Yukawa and HS to hard sphere.

### C. Thermal conduction

The thermal conductivity will be denoted by  $\lambda$ . The definitions of normalized thermal conductivities are given by  $\lambda' = \lambda/\lambda_{pf}$  [23],  $\lambda^* = \lambda/\lambda_{ef}$ , and  $\lambda^r = \lambda/\lambda_{mic}$  [17,18,72,77], where  $\lambda_{pf} = k_B \rho_i \omega_p a_{WS}^2$ ,  $\lambda_{ef} = k_B \rho_i \sqrt{3} \omega_e a_{WS}^2$ , and  $\lambda_{mic} = \rho_i^{2/3} k_B \sqrt{k_B T/m}$ . Here,  $\lambda_{mic}$  is the macroscopic thermal conductivity [17,18,72,77]. Note that  $\lambda^* = \lambda'$  when  $\kappa=0$ . The normalization used for  $\lambda^*$  may be considered to be a natural extension of  $\lambda'$  of the OCP in finite screening.

To our knowledge, no systematic MD calculations over a wide range of the system parameters  $\{\Gamma, \kappa\}$  have been carried out [21,22,81,82]. We have thus decided to keep the formula found [14] by fitting the most recent and accurate MD data for the OCP system of Donko and Nyiri [81] by the same form selected by Saigo and Hamaguchi for shear viscosity [20]. Assuming a quasiuniversal behavior, we can estimate the Yukawa thermal conductivity from

$$\lambda^*(\Gamma, \kappa) = 0.01176T^* + \frac{0.881}{T^*} + 0.1655, \quad (58)$$

where  $T^*$  is the normalized temperature already encountered.

The situation is less dramatic for HS system because the deviations of MD calculations from the Enskog's expression have been proven to be barely perceptible within the few percent accuracy of the data [81]. As a consequence, once the effective hard-sphere packing fraction  $\eta$  of the Yukawa system is obtained using the VMHNC method, the Yukawa thermal conductivity normalized in terms of  $\lambda_{ef}$  may be estimated from the HS result  $\lambda_{HS}$  as

$$\lambda_{YHS}^*(\Gamma, \kappa) \equiv \frac{\lambda_{HS}}{\lambda_{ef}} = \frac{\lambda_{HS}}{\lambda_E} \frac{\lambda_E}{\lambda_{gas}} \frac{\lambda_{gas}}{\lambda_{ef}}, \quad (59)$$

where

$$\begin{aligned} \frac{\lambda_{HS}}{\lambda_E} &= 1, \\ \frac{\lambda_E}{\lambda_{gas}} &= \left[ \frac{(1-\eta)^3}{(1-\eta/2)} + 1.200(4\eta) + 0.755(4\eta)^2 \frac{(1-\eta/2)}{(1-\eta)^3} \right], \end{aligned} \quad (60)$$

$$\frac{\lambda_{gas}}{\lambda_{ef}} = \frac{25}{64\sqrt{3}\eta^{2/3}} \sqrt{\frac{\pi}{\Gamma}} e^{0.2058\kappa^{1.590}}.$$

Here,  $\lambda_{gas}$  and  $\lambda_E$  are the results for a dilute gas and the Enskog's result, respectively. Note that the CS equation of state for the radial pair distribution function at contact has been used [14]. In Eq. (59), Y refers to Yukawa and HS to hard sphere.

### D. Rosenfeld approach

A semiempirical "universal" corresponding-states relationship, for the dimensionless transport coefficients of dense fluids as functions of the reduced configurational entropy, has been proposed by Rosenfeld [17], extended to dilute fluids by the same author [18], and established by many simulations [17,83]. This approach is invaluable for four reasons. First, an accurate, theoretically based, approach to dense-fluid transport coefficients is still lacking. Second, no convergent perturbation theory of transport coefficients has been established. Third, the brute-force computer methods can be used to estimate transport coefficients, but these methods are considerably too time consuming, for the same accuracy, than those designed to measure equilibrium properties and cannot be considered as black-box routines that generate data intensively over an industrialized scale. Fourth, this analytical relation between transport coefficients and excess entropy allows us to estimate, for instance, self-diffusion, shear viscosity, and thermal conductivity from the equation of state of monatomic fluids with arbitrary pair potentials. In summary, one realizes all the benefits of the Rosenfeld approach to estimate transport coefficients knowing only the excess entropy of the system of interest. This method is as useful as Enskog's original recipe relating transport coefficients to thermal pressure [84].

Let us consider a one-component fluid with a reduced excess entropy  $s = -S/(Nk_B)$ , where  $S$  is the entropy of the system of interest composed of  $N$  particles in the volume  $\Omega$  at temperature  $T$ . In short,  $s$  is equal to minus the reduced excess or configurational entropy over the ideal-gas value. The quasiuniversal behavior for the transport coefficients has been derived either from many simulations for dense fluids [17] or from the Enskog's theory for dilute fluids [18] by considering, i.e., normalized self-diffusion  $D^r$ , normalized shear viscosity  $\eta^r$ , and normalized thermal conductivity  $\lambda^r$ . Keeping the aforementioned normalization in terms of

Einstein frequency to be consistent with the MD of Hamaguchi *et al.*, the Rosenfeld scaling entropy transport coefficients of self-diffusion  $D_{esc}^*$ , shear viscosity  $\eta_{esc}^*$ , and thermal conductivity  $\lambda_{esc}^*$  for Yukawa fluid are given by

$$\begin{aligned} D_{esc}^* &= D^r \frac{D_{md}}{D_{ef}}, \\ D_{esc}^* &= \eta^r \frac{\eta_{mv}}{\eta_{ef}}, \\ \lambda_{esc}^* &= \lambda^r \frac{\lambda_{mtc}}{\lambda_{ef}}, \end{aligned} \quad (61)$$

where

$$\frac{D_{md}}{D_{ef}} = \sqrt{3} \frac{\eta_{mv}}{\eta_{ef}} = \sqrt{3} \frac{\lambda_{mtc}}{\lambda_{ef}} = \frac{e^{0.2058\kappa^{1.590}}}{\sqrt{\Gamma}} \left( \frac{4\pi}{3} \right)^{1/3}. \quad (62)$$

Note that normalizing the self-diffusion by  $D_{ef} = \sqrt{3}\omega_e a_{WS}^2$  instead of  $D_{ef} = \sqrt{3}\omega_e a_{WS}^2$  as proposed originally [19] would lead to the simpler and more symmetric expression

$$\frac{D_{md}}{D_{ef}} = \frac{\eta_{mv}}{\eta_{ef}} = \frac{\lambda_{mtc}}{\lambda_{ef}} = \frac{e^{0.2058\kappa^{1.590}}}{\sqrt{3\Gamma}} \left( \frac{4\pi}{3} \right)^{1/3}. \quad (63)$$

We have kept however the original normalization for the sake of consistency with literature. For dense fluids [18],

$$\begin{aligned} D^r &\approx 0.6e^{-0.8s}, \\ \eta^r &\approx 0.2e^{0.8s}, \\ \lambda^r &\approx 1.5e^{0.5s}, \end{aligned} \quad (64)$$

whereas for dilute fluids [18], we obtain for HS

$$\begin{aligned} D^r &\approx 0.37s^{-2/3}, \\ \eta^r &\approx 0.27s^{-2/3}, \\ \lambda^r &\approx \frac{15}{4}\eta^r, \end{aligned} \quad (65)$$

and for OCP

$$\begin{aligned} D^r &\approx \frac{0.40s^{-4/3}}{\ln \left[ 1 + \left( \frac{2}{3s} \right)^2 \right]}, \\ \eta^r &\approx \frac{0.35s^{-4/3}}{\ln \left[ 1 + \left( \frac{2}{3s} \right)^2 \right] - \frac{1}{1 + \left( \frac{3s}{2} \right)^2}}, \\ \lambda^r &\approx \frac{15}{4}\eta^r. \end{aligned} \quad (66)$$

The quasiuniversal behavior for dense fluids, which holds also for the OCP case, is replaced by two different behaviors that depend on the inverse power law of the pair potential for dilute fluids [18].

## E. Numerical results

The elegant and deep method proposed by Rosenfeld relates the transport coefficients to the equation of state. We have thus used the VMHNC reduced excess entropy to see how the predictions of Eqs. (64) and (52) for self-diffusion and shear viscosity compare to MD simulations (52) and (55), and to the self-diffusion and shear viscosity of the HS system given by Eqs. (53) and (56) using the effective HS packing fraction  $\eta_{eff}$  of the VMHNC theory. Results are plotted in Fig. 7 (Fig. 11), Fig. 8 (Fig. 12), Fig. 9 (Fig. 13), and Fig. 10 (Fig. 14), where the self-diffusion coefficient  $D^*$  (the shear viscosity  $\eta^*$ ), normalized in terms of Einstein frequency, is plotted in function of normalized temperature  $T^*$  for  $\kappa=0$ ,  $\kappa=1$ ,  $\kappa=3$ , and  $\kappa=5$ , respectively. The quasiuniversal entropy scaling formulas for dilute and dense HS fluids proposed by Rosenfeld [17,18] are compared to MD calculations of Ohta (Saigo) and Hamaguchi for self-diffusion coefficient (shear viscosity) [19] (Ref. [20]). The range of variation of  $T^*$  is taken from Ref. [20]. It covers strongly and weakly coupled Yukawa systems and corresponds roughly to Yukawa system excess entropy above and below one, respectively. First, we can see that the effective HS system is very efficient to estimate self-diffusion and shear viscosity. In both cases, the agreement with MD calculations improves with increasing  $\kappa$ , denoting the tendency of the Yukawa system to be more HS-like at strong screening [14]. Note that the VMHNC theory tends towards the HNC approximation at large  $T^*$ , i.e., for uncoupled plasma. The Bridge function becomes irrelevant in that limit, and one cannot use the effective HS packing fraction  $\eta_{eff}$  of the VMHNC theory for very large values of  $T^*$ , i.e., typically for  $T^* > 10^3$ . This explains the systematic deviation of the calculations using the effective HS notion with respect to MD results for weak screening at large  $T^*$ . Second, MD calculations nicely interpolate between dilute fluid at high  $T^*$  and dense fluid at low  $T^*$ , the transition between both regimes being located between  $T^* = 10$  and  $T^* = 100$ . One could even predict a minimum for shear viscosity [14,77]. Since excess entropy remains well defined when the VMHNC theory reduces to the HNC approach, one can use the Rosenfeld method even for large values of  $T^*$ .

## V. STRUCTURE FUNCTIONS

Among the various structure functions that can be obtained with the VMHNC theory, the radial pair distribution function  $g(r)$ , the structure factor  $S(k)$ , and the screening potential  $H(r)$  deserve particular attention.  $S(k)$  is simply related to the Fourier transform of the pair correlation function  $h(r) = g(r) - 1$ ,

$$S(k) = 1 + \rho_{ion} \tilde{h}(k), \quad (67)$$

whereas  $H(r)$  is defined in terms of the pair interaction potential and the pair distribution function. For YOCP system, we have

$\kappa=0$

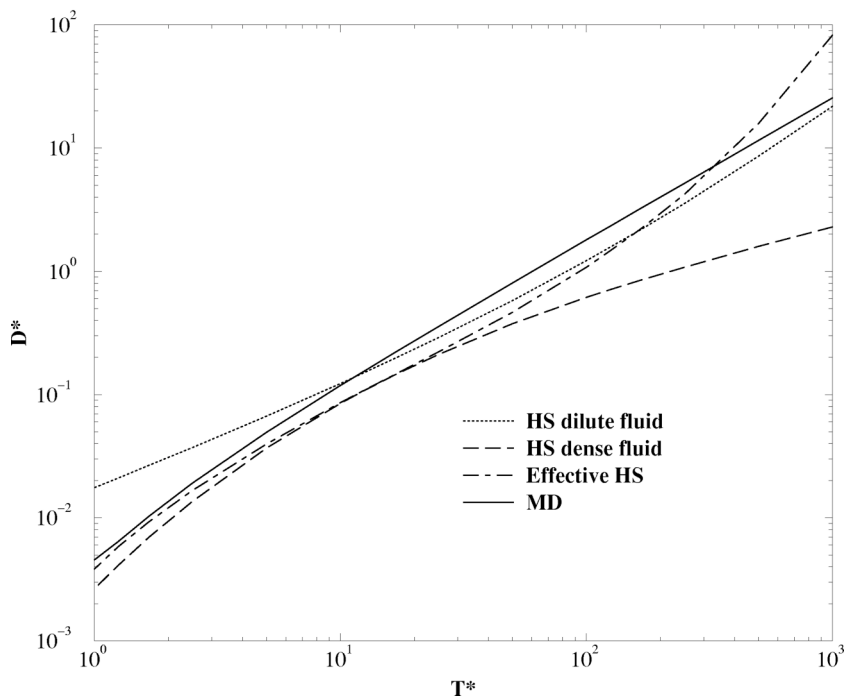


FIG. 7. Self-diffusion coefficient normalized in terms of Einstein frequency  $D^*$  vs normalized temperature  $T^*$  of the Yukawa system with  $\kappa=0$ . The quasiuniversal entropy scaling formulas for dilute and dense HS fluids proposed by Rosenfeld [17,18] are compared to MD calculations of Ohta and Hamaguchi [19] and to the effective HS using the analytic formula of Erpenbeck and Wood [18,78].

$$H(r) = \ln[g(r)] + \frac{\Gamma}{r} e^{\kappa r} \quad (68)$$

in  $a_{WS}$  units. In the same units,  $S(k) = 1 + (3/4\pi)\tilde{h}(k)$ .

$g(r)$  plays a central role in the theory of fluid since it enters in the determination of the equation of state and in the estimation of transport coefficients through the excess en-

tropy or the effective hard-sphere parameter  $\eta_{eff}$ . Note that it can also be used to determine the nearest-neighbor distribution function either directly [85], or indirectly using known properties of the HS reference system concerning nearest-neighbor statistics for packings of hard spheres [86,87]. Indeed, two different but closely related nearest-neighbor distribution functions  $H_p(r)$  and  $H_v(r)$  can be defined. They

$\kappa=1$

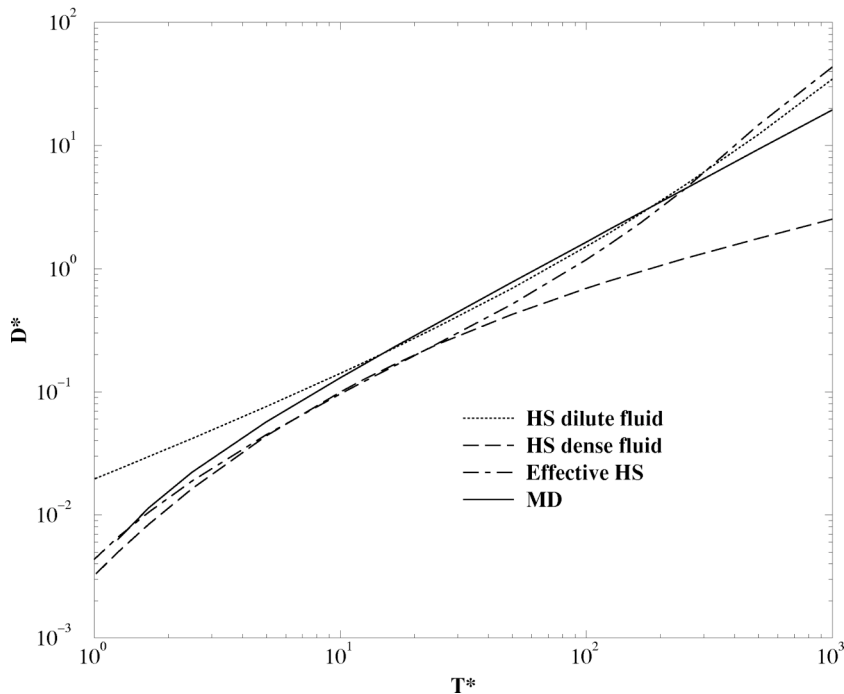


FIG. 8. Self-diffusion coefficient normalized in terms of Einstein frequency  $D^*$  vs normalized temperature  $T^*$  of the Yukawa system with  $\kappa=1$ . The quasiuniversal entropy scaling formulas for dilute and dense HS fluids proposed by Rosenfeld [17,18] are compared to MD calculations of Ohta and Hamaguchi [19] and to the effective HS using the analytic formula of Erpenbeck and Wood [18,78].

$\kappa=3$

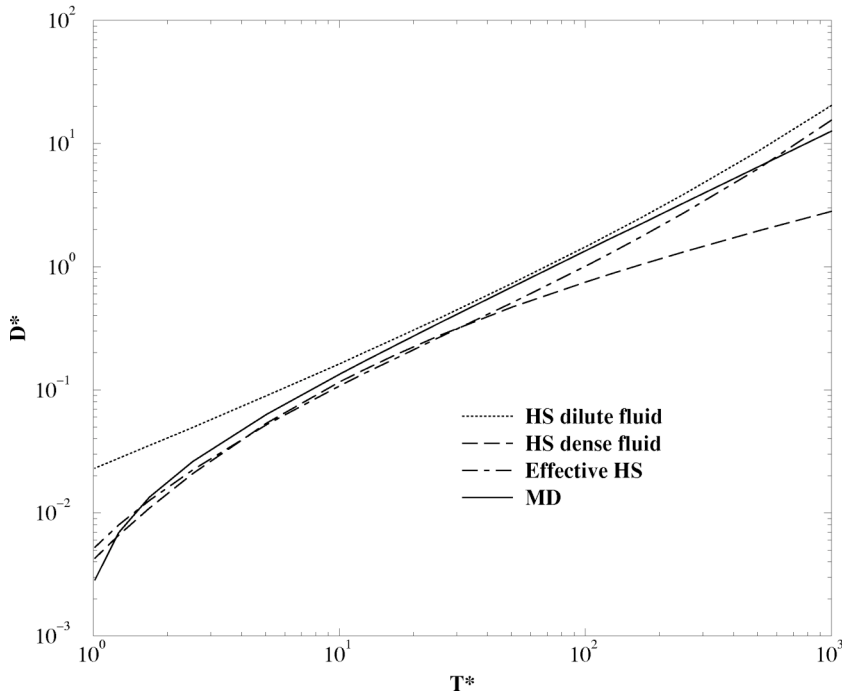


FIG. 9. Self-diffusion coefficient normalized in terms of Einstein frequency  $D^*$  vs normalized temperature  $T^*$  of the Yukawa system with  $\kappa=3$ . The quasiuniversal entropy scaling formulas for dilute and dense HS fluids proposed by Rosenfeld [17,18] are compared to MD calculations of Ohta and Hamaguchi [20] and to the effective HS using the analytic formula of Erpenbeck and Wood [18,78].

only differ by the presence or the absence of a particle at the chosen arbitrary reference point. It could be rather challenging to compare the predictions of the VMHNC to MC or MD simulations using analytical formulas for the void  $H_v(r)$  and particle  $H_p(r)$  densities involving  $\eta_{eff}$ . One could thus bring some answer to the fundamental query of studying the effect of the nearest neighbor on some reference particle in the

system for Yukawa system first, and by extension, for many different kinds of pair potential, owing to the flexibility of the VMHNC theory. Curiously, the quantity that is determined from scattering experiments is, however,  $S(k)$ . But both  $g(r)$  and  $S(k)$  enter explicitly in the study of excitation and propagation of waves in dusty plasmas, as illustrated, for instance, by the QLCA. We have performed extensive calcu-

$\kappa=5$

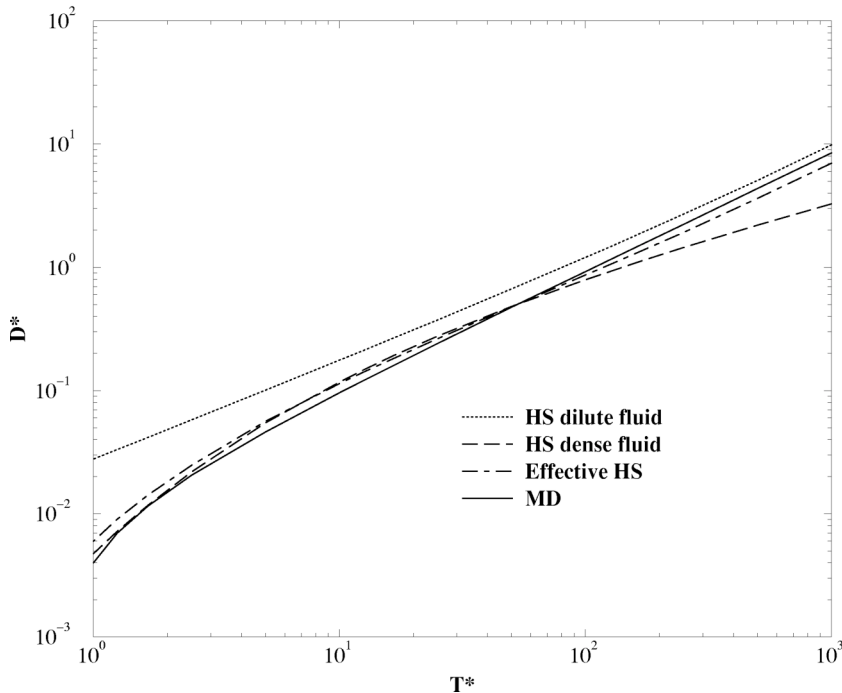


FIG. 10. Self-diffusion coefficient normalized in terms of Einstein frequency  $D^*$  vs normalized temperature  $T^*$  of the Yukawa system with  $\kappa=5$ . The quasiuniversal entropy scaling formulas for dilute and dense HS fluids proposed by Rosenfeld [17,18] are compared to MD calculations of Ohta and Hamaguchi [19] and to the effective HS using the analytic formula of Erpenbeck and Wood [18,78].

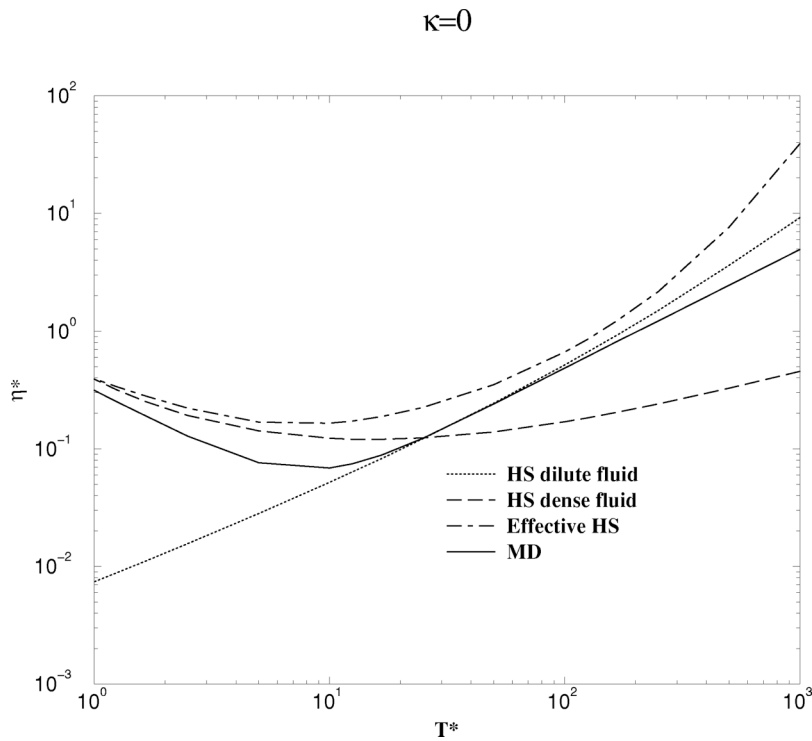


FIG. 11. Shear viscosity normalized in terms of Einstein frequency  $\eta^*$  vs normalized temperature  $T^*$  of the Yukawa system with  $\kappa=0$ . The quasiuniversal entropy scaling formulas for dilute and dense HS fluids proposed by Rosenfeld [17,18] are compared to MD calculations of Saigo and Hamaguchi [20] and to the effective HS using an analytic formula [18,23,80].

lations for  $g(r)$  and  $S(k)$  using the VMHNC approach at various values of  $t^*$  for integer  $\kappa \in [0, 5]$ . As expected, we find that the most striking feature is the similarity known as the Hansen-Verlet rule concerning the height of the first peak of  $S(k)$  near freezing [71]. Moreover,  $S(k)$  becomes nearly independent of  $\kappa$  near the liquid-solid phase boundary. However, no other universal trend can be observed concerning either  $S(k)$  or  $g(r)$  and screening can have an important effect at low  $t^*$ .

The properties of the screening potential  $H(r)$  are unfortunately too often overlooked. This may be explained by the fact that  $H(r)$  takes values in the region close to origin, where the potential is very highly repulsive and where the resulting  $g(r)$  takes on very small values (practically zero in fact). The probability for very close encounters is essentially zero and  $H(r)$  is thus of delicate access by MC or MD simulations [35,69]. However, the behavior of  $H(r)$  at short separation plays an essential role in estimating the enhancement

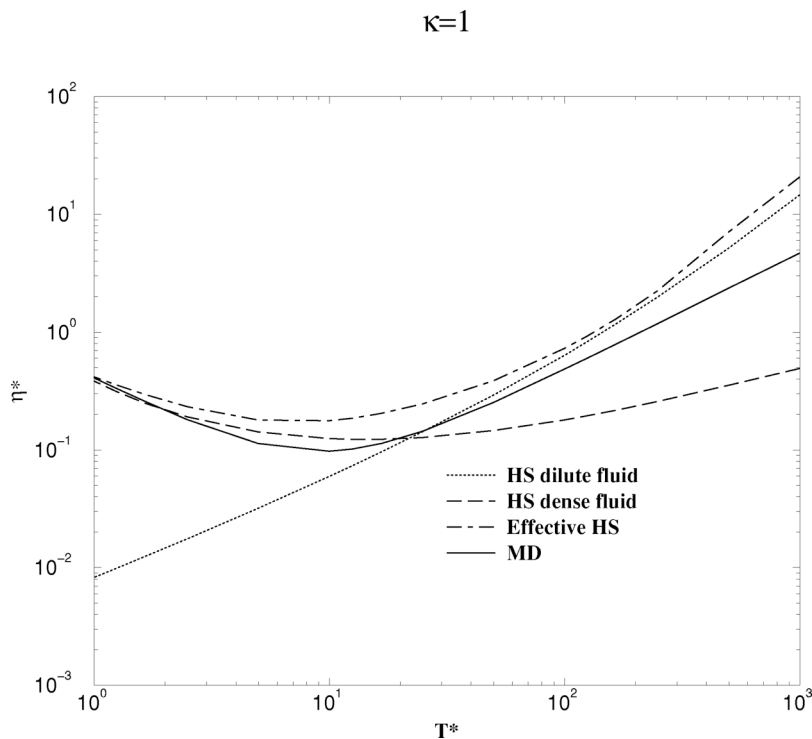


FIG. 12. Shear viscosity normalized in terms of Einstein frequency  $\eta^*$  vs normalized temperature  $T^*$  of the Yukawa system with  $\kappa=1$ . The quasiuniversal entropy scaling formulas for dilute and dense HS fluids proposed by Rosenfeld [17,18] are compared to MD calculations of Saigo and Hamaguchi [20] and to the effective HS using an analytic formula [18,23,80].

$\kappa=3$

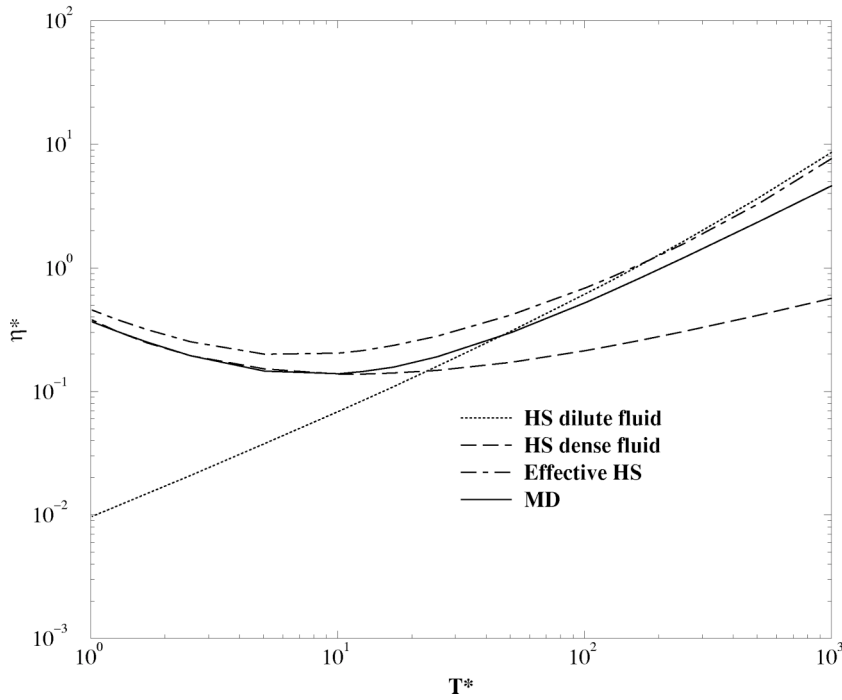


FIG. 13. Shear viscosity normalized in terms of Einstein frequency  $\eta^*$  vs normalized temperature  $T^*$  of the Yukawa system with  $\kappa=3$ . The quasiuniversal entropy scaling formulas for dilute and dense HS fluids proposed by Rosenfeld [17,18] are compared to MD calculations of Saigo and Hamaguchi [20] and to the effective HS using an analytic formula [18,23,80].

factors of thermonuclear reaction rates and in studying the influence of screening from bare Coulomb to Yukawa pair interaction. Moreover,  $H(r)$  plays a key role in the study of the short-range behavior of Bridge functions. Finally, the zero separation theorem for the screening potentials [88–90] provides an important consistency test for approximate theories of the equation of state of fluid mixtures [69].

The pair correlation function can be expressed through the free energy change upon fixing the positions of the pair of

fluid particles in the appropriate configuration to form an interaction-site molecule, so that [35]

$$H(r) = -[f_1^{ex}(r) - f_0^{ex}] + \frac{\Gamma}{r} e^{\kappa r}. \quad (69)$$

In this expression,  $f_0^{ex}$  is the excess free energy per particle in units of  $k_B T$  of the  $N$ -particle system in the presence of a uniform neutralizing background and  $f_1^{ex}(r)$  is that of the

$\kappa=5$

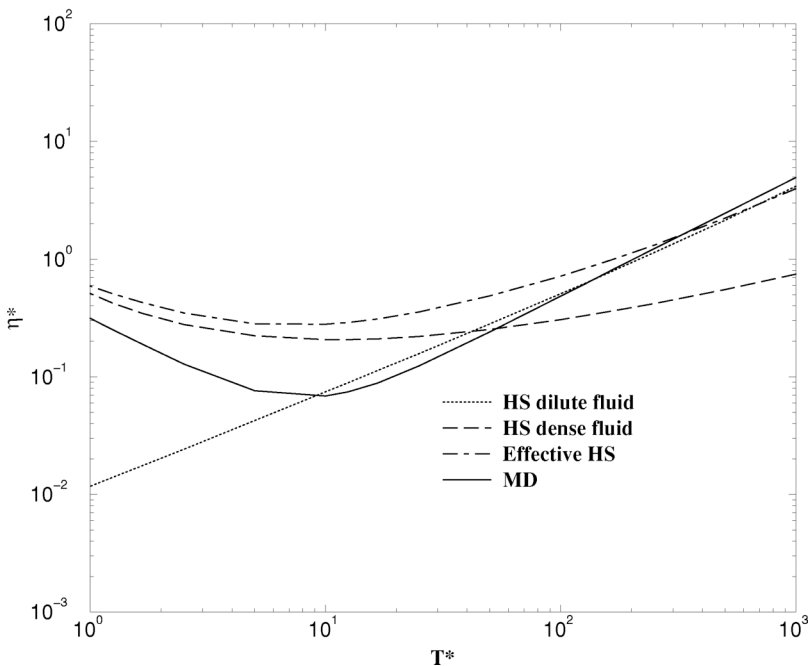


FIG. 14. Shear viscosity normalized in terms of Einstein frequency  $\eta^*$  vs normalized temperature  $T^*$  of the Yukawa system with  $\kappa=5$ . The quasiuniversal entropy scaling formulas for dilute and dense HS fluids proposed by Rosenfeld [17,18] are compared to MD calculations of Saigo and Hamaguchi [20] and to the effective HS using an analytic formula [18,23,78].

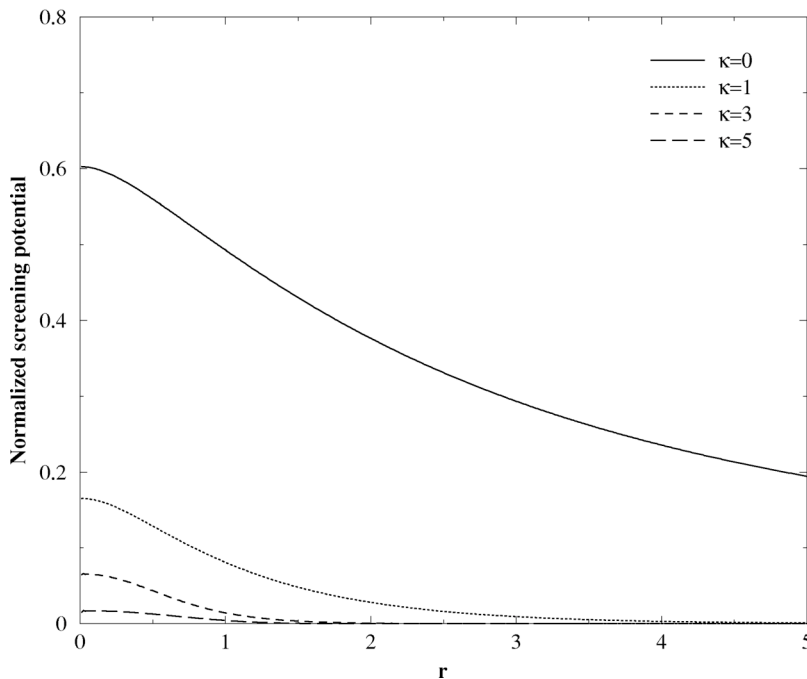
**$t^*=0.001$** 

FIG. 15. Normalized screening potential  $H(r)/\Gamma$  in function of  $r$  in  $a_{WS}$  units from the VMHNC theory for  $\kappa=0, 1, 3, 5$  and inverse normalized temperature  $t^*=0.001$ .

same system but with the pair of particles kept at fixed separation  $r$ , forming a two-site charge cluster in the presence of both the remaining  $(N-2)$ -particle system and the uniform neutralizing background. Since  $f_1^{ex}(r)$  already contains the intramolecular interaction  $(\Gamma/r)e^{\kappa r}$ ,  $H(r)$  is finite as  $r \rightarrow 0$ . According to Widom [90],  $H(r)$  can be expanded in even powers around  $r=0$  with polynomial coefficients of alternate signs,

$$H(r) = H_0 - H_1 r^2 + H_2 r^4 - H_3 r^6 + O(r). \quad (70)$$

The coefficients  $H_0, \dots, H_3$  are sufficient to determine  $H(r)$  for  $r \in [0, 1]$ , i.e., when we have nearly no information about  $g(r)$ , but they are very difficult to obtain in the most general case [36]. As for OCP however,  $H_1 = \Gamma/4$  [90] and  $H_0$  is nearly known. Indeed,  $H_0$  can be estimated combining Eq. (69) and the linear-mixing rule for binary ionic mixture. This approximation is known to be very accurate for strongly coupled plasmas [35,36,69,91]. This method has been proven to be very good for YOCP too [35,3]. Using the excess free energy  $f_Y^{ex}$  of the Yukawa system [35],

$$H_0 \approx 2f_Y^{ex}(\Gamma, \kappa) - f_Y^{ex}(2^{5/3}\Gamma, 2^{1/3}\kappa). \quad (71)$$

As above, two methods can be employed to calculate  $f_Y^{ex}$ , namely, the analytical fits of the MD results of Hamaguchi *et al.* [11–13] or the VMHNC itself. This fact constitutes another stringent test of the internal consistency of the theory because  $H_0$  requires the excess free energy at two points inside the Yukawa plane, one of them not necessarily inside the fluid domain. It is a kind of nonlocal test of an essentially local approach. Owing to this particularity of the VMHNC theory, the calculations are rather straightforward, as explained above.

Since the PYHS Bridge function is linear and negative at the origin, it is by no means trivial that the VMHNC will give a well-behaved screening potential around the origin. We have plotted  $H(r)/\Gamma$  obtained by the VMHNC theory at  $t^*=0.001, 0.01, 0.1, 1$  for integer  $\kappa \in [0, 5]$  in Figs. 15–18. First, the screening can have dramatic impact on  $H(r)$  values near the origin. For instance,  $H(0)/\Gamma$  can be reduced to more than one order of magnitude from  $\kappa=0$  to  $\kappa=5$ . Second, the zero-separation law is satisfied for  $t^*=0.0001$ , approximately for  $t^*=0.01$ , but not for  $t^*=0.1$  and  $t^*=1$ . When we go from low to high values of  $T^*$ , the screening potential deviates progressively from the general Taylor expansion given by Eq. (70). This indicates that the linear behavior of the PYHS Bridge function is responsible for such a feature and contradicts the plausible fact that both the direct correlation function and the Bridge function behave essentially as the screening potential near the origin [41]. Yet, the shape of  $H(r)/\Gamma$  is nearly linear over the region  $[r: g(r) > 10^{-3}, r: g(r) = \max]$ , a feature shared also by the HS system [41]. As already enhanced by Rosenfeld *et al.* [41], these conflicting tendencies do not prevent the search of universal characteristics, because the region where the feature is distinct is obviously the region where for computational purposes the Bridge function is undefined. As a practical point of view, what does it mean? Maybe we expect too much from the VMHNC theory that has been proven so successful so far to describe such a complicated system as YOCP with long-range and short-range characteristics and with correlated and uncorrelated features, depending on the coupling and screening parameters. Since the behavior of the Bridge function is ill defined near the origin, we could imagine to introduce a tiny correction to the Bridge function such that the screening potential satisfies the Widom expansion (70). This can be viewed as an attempt to minimize the VMHNC excess free energy under the con-

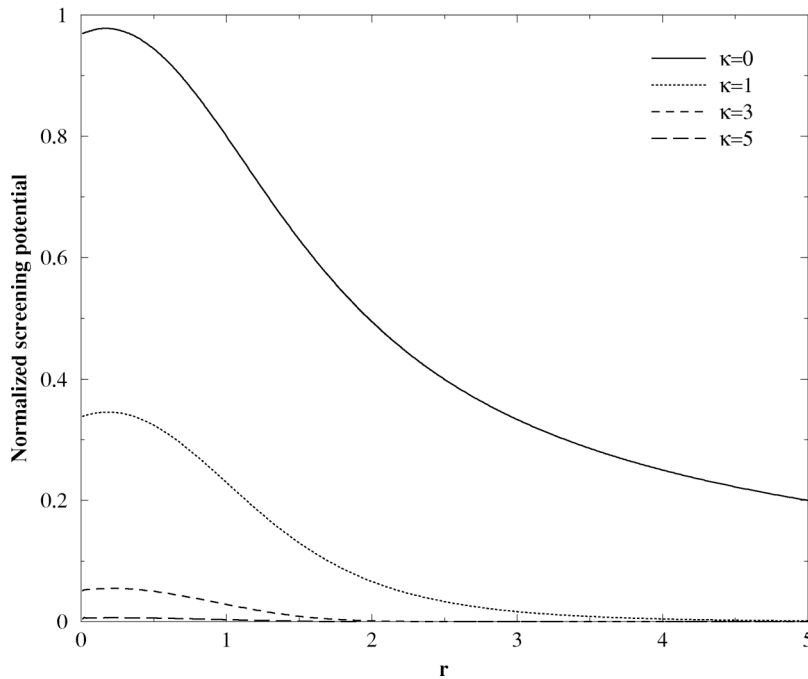
**$t^*=0.01$** 

FIG. 16. Normalized screening potential  $H(r)/\Gamma$  in function of  $r$  in  $a_{WS}$  units from the VMHNC theory for  $\kappa=0,1,3,5$  and inverse normalized temperature  $t^*=0.01$ .

straint of satisfying the zero-separation theorem. Last but not the least, note that it appears intriguing that the undefined values of the Bridge function near the origin have negligible effects on the structure function, thermodynamic quantities, and transport coefficients, as long as the PYHS Bridge function is employed, whereas these values are intimately connected to excess free energy difference of two Yukawa sys-

tems  $\{\Gamma, \kappa\}$  and  $\{2^{5/3}\Gamma, 2^{1/3}\kappa\}$  at the same time.

Since such modifications of the VMHNC theory are beyond the scope of this paper, we have tried to estimate  $H_0$ ,  $H_1$ , and  $H_2$  of Eq. (70) using the method proposed by Rosenfeld [35] to extrapolate the MC data for the OCP screening potential made zero, given the simulations data in the range  $[r_{min}, 2]$  in  $a_{WS}$  units, where  $r_{min} \approx 1$  for  $\Gamma \approx 160$  and  $r_{min}$

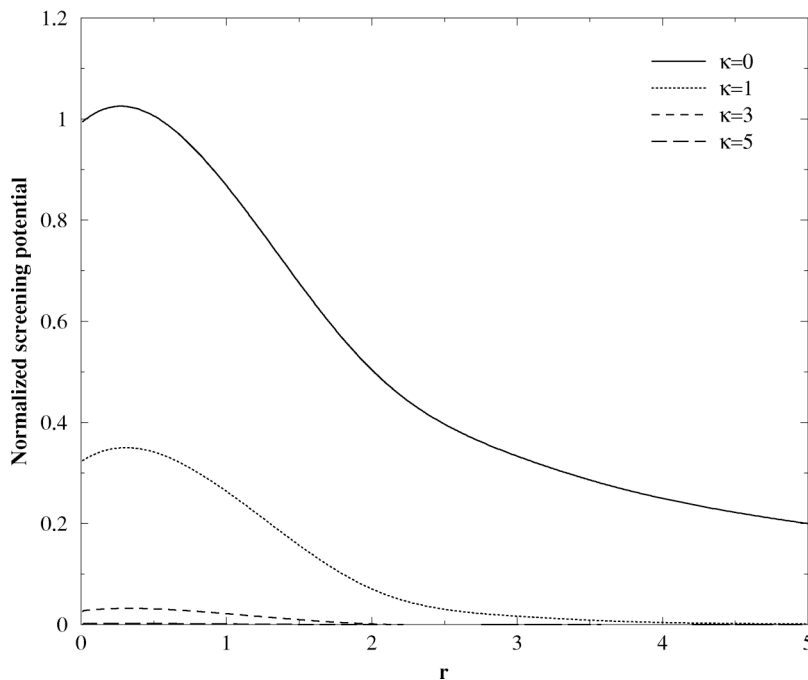
 **$t^*=0.1$** 

FIG. 17. Normalized screening potential  $H(r)/\Gamma$  in function of  $r$  in  $a_{WS}$  units from the VMHNC theory for  $\kappa=0,1,3,5$  and inverse normalized temperature  $t^*=0.1$ .

$$t^*=1$$

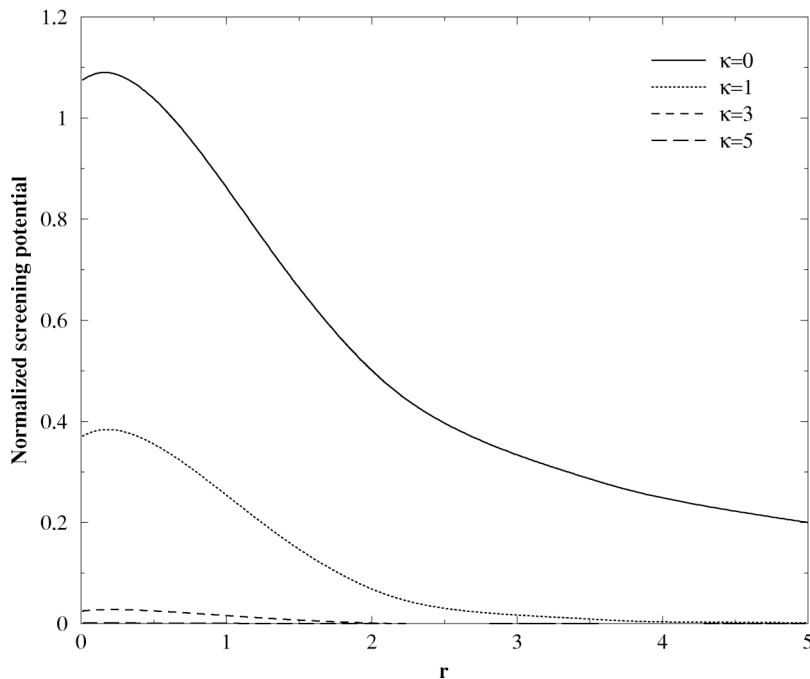


FIG. 18. Normalized screening potential  $H(r)/\Gamma$  in function of  $r$  in  $a_{WS}$  units from the VMHNC theory for  $\kappa=0,1,3,5$  and inverse normalized temperature  $t^*=1$ .

$\approx 0.5$  for  $\Gamma \approx 10$ . This is performed after solving the MHNC equations with the usual PYHS Bridge function. Using Eq. (70),  $H(r)$  can be written as

$$H(r)/\Gamma = \begin{cases} h_0 - h_1 r^2 + h_2 r^4 & \text{for } r \leq r_0 \\ f(r) & \text{for } r \geq r_0, \end{cases} \quad (72)$$

where  $f(r)$  represents  $H(r)/\Gamma$  obtained from the VMHNC theory and expanded in Chebyshev polynomials. The four unknown parameters  $h_0$ ,  $h_1$ ,  $h_2$ , and  $r_0$  are determined requiring that the function and its first three derivatives are continuous at  $r_0$ :

$$\begin{aligned} f(r_0) &= h_0 - h_1 r_0^2 + h_2 r_0^4, \\ f'(r_0) &= -2h_1 r_0 + 4h_2 r_0^3, \\ f''(r_0) &= -2h_1 + 12h_2 r_0^2, \\ f'''(r_0) &= 24h_2 r_0. \end{aligned} \quad (73)$$

Equations (73) generalize Eqs. (10) of Ref. [35] to consider the case in which  $h_1$  is not assumed to be already known. We have compared in Table II our predictions of the VMHNC method (Rosenfeld) with respect to the values, extracted from the MD simulations [11–13] (Jancovici<sup>a</sup>) or from the VMHNC theory (Jancovici<sup>b</sup>) using Eq. (71). For simplicity, we have taken  $r_{min}=0.5$ , i.e., we have assumed that the screening potential calculated by the VMHNC theory in the interval  $[0.5, 2]$  for all values of  $\Gamma$  is known. Since  $H_1 = \Gamma/4$  for OCP, we tried to mimic exactly what Rosenfeld did in Ref. [35] by looking for solutions of his set of Eqs. (10) at fixed  $H_1$ . However, we did not find any solutions. So, we were forced to look for solutions of Eqs. (73) with  $H_1$  as a

TABLE II. Screening potentials for the one-component plasma. The extrapolation method of Rosenfeld [Rosenfeld, Eq. (73)] is compared to the Jancovici method [Eq. (71)] using the fits to the MD results of Hamaguchi *et al.* [11–13] (Jancovici<sup>a</sup>) and the VMHNC theory (Jancovici<sup>b</sup>).

$\Gamma$	$r_0$	Rosenfeld			Jancovici <sup>a</sup>	Jancovici <sup>b</sup>
		$h_2$	$h_1$	$h_0$	$h_0$	$h_0$
10.000	1.420	0.021	0.223	1.072	1.099	1.099
20.000	1.103	0.021	0.221	1.069	1.095	1.096
30.000	1.017	0.024	0.230	1.072	1.091	1.092
40.000	0.975	0.027	0.239	1.076	1.088	1.088
50.000	0.930	0.030	0.246	1.080	1.085	1.086
60.000	0.895	0.032	0.253	1.084	1.083	1.084
70.000	0.884	0.034	0.259	1.088	1.082	1.082
80.000	0.871	0.036	0.264	1.091	1.080	1.081
90.000	0.788	0.038	0.268	1.094	1.079	1.080
100.00	0.785	0.040	0.273	1.096	1.078	1.078
110.00	0.789	0.041	0.276	1.098	1.077	1.077
120.00	0.788	0.042	0.280	1.101	1.076	1.077
130.00	0.786	0.043	0.283	1.103	1.076	1.076
140.00	0.783	0.044	0.285	1.105	1.075	1.075
150.00	0.691	0.046	0.289	1.106	1.074	1.074
160.00	0.687	0.047	0.290	1.108	1.074	1.073
170.00	0.683	0.048	0.294	1.109	1.073	1.071
180.00	0.680	0.049	0.295	1.111	1.073	1.070

free parameter too. As seen in Table II, results are not bad. The matching point  $r_0$  and  $h_2=H_2/\Gamma$  decrease with increasing  $\Gamma$  and  $h_2$  remains small. However,  $h_1=H_1/\Gamma$  departs notably from the nominal value 0.25 and  $h_0=H_0/\Gamma$  has the wrong behavior with increasing  $\Gamma$  and remains notably around 1.1. Compared to Jancovici<sup>a</sup> reference calculations, discrepancies may reach 2%. Note that our updated Jancovici's original expression [90] using the fits of MD results [11–13], i.e., Jancovici<sup>a</sup>, gives results identical to the ones given by Rosenfeld in Table I of Ref. [35] using the most accurate fit to the best OCP MC data at the time. As for our updated Jancovici's original expression [90] using directly the VMHNC theory, i.e., Jancovici<sup>b</sup>, we can see that the predicted values for  $h_0$  are nearly identical with the reference calculations denoted by Jancovici<sup>a</sup>.

What can explain these facts? It is clear that the linear behavior of the PYHS Bridge function is one cause. Another reason may be simply the overall VMHNC theory strategy itself, which stands on a variational principle to calculate the excess free energy of the YOCP system. As usual, there is no guarantee that this method will produce reliable estimate of a quantity other than excess free energy, especially where no reference is made to a particular quantity we want to calculate during the minimization process. The VMHNC is very powerful where it has been designed to be so, and does its best where nothing could be expected from it *a priori*. It is clearly challenging to try to solve the VMHNC under constraint, i.e., by respecting the Widom expansion (70).

## VI. CONCLUSION

The VMHNC theory has been used to study the Yukawa system over the entire fluid domain for a wide range of the

system parameters  $\{\Gamma, \kappa\}$ . A variational method has been presented to speed up the resolution of the MHNC integral equations at strong coupling. The liquid-solid phase boundary of the Yukawa system can be reproduced with a very good accuracy using three different freezing indicators, i.e., the Hansen-Verlet rule, the Bridge freezing rule, or the freezing properties of the effective hard-sphere system that enters in the VMHNC theory. The screening potential can be estimated with good accuracy, except in the vicinity of the origin where the Widom expansion breaks down for strong coupling. Explanations and solutions have been proposed to remedy this tiny defect. Extensive comparisons with simulation results have shown that the VMHNC approach is very powerful to calculate equation of state quantities, i.e., pressure, internal energy, free energy, and entropy. It has been proven that this method can also be very efficient to estimate transport coefficients, i.e., self-diffusion, shear viscosity, and thermal conductivity. One can employ either the known transport coefficients of the HS system or the quasiuniversal entropy scaling of Rosenfeld based on a correspondence between transport coefficients and reduced excess entropy.

The method presented here can be extended to other systems and to other properties for which expressions are known for the hard-sphere system. The same method can be applied to mixtures.

## ACKNOWLEDGMENT

The author thanks D. Gogny for helpful discussions and constant support.

- 
- [1] P. K. Shukla, *Phys. Plasmas* **8**, 1791 (2001).
  - [2] S. Ichimaru, *Statistical Plasma Physics, Volume II: Condensed Plasmas* (Addison-Wesley, New York, 1994).
  - [3] Y. Rosenfeld and G. Chabrier, *J. Stat. Phys.* **89**, 283 (1997).
  - [4] R. O. Rosenberg and D. Thirumalai, *Phys. Rev. A* **33**, 4473 (1986).
  - [5] K. Kremer, M. O. Robbins, and G. S. Grest, *Phys. Rev. Lett.* **57**, 2694 (1986).
  - [6] M. O. Robbins, K. Kremer, and G. S. Grest, *J. Chem. Phys.* **88**, 3286 (1988).
  - [7] T. C. Killian, S. Kulin, S. D. Bergeson, L. A. Orozco, C. Orzel, and S. L. Rolston, *Phys. Rev. Lett.* **83**, 4776 (1999).
  - [8] S. Kulin, T. C. Killian, S. D. Bergeson, and S. L. Rolston, *Phys. Rev. Lett.* **85**, 318 (2000).
  - [9] U. Konopka, G. E. Morfill, and L. Ratke, *Phys. Rev. Lett.* **84**, 891 (2000).
  - [10] J. M. Caillol and D. Gilles, *J. Stat. Phys.* **100**, 905, 933 (2000).
  - [11] S. Hamaguchi and R. T. Farouki, *J. Chem. Phys.* **101**, 9876, 9885 (1994).
  - [12] S. Hamaguchi, R. T. Farouki, and D. H. E. Dubin, *J. Chem. Phys.* **105**, 7641 (1996).
  - [13] S. Hamaguchi, R. T. Farouki, and D. H. E. Dubin, *Phys. Rev. E* **56**, 4671 (1997).
  - [14] G. Faussurier and M. S. Murillo, *Phys. Rev. E* **67**, 046404 (2003).
  - [15] S. Galam and J. P. Hansen, *Phys. Rev. A* **14**, 816 (1976).
  - [16] B. Firey and N. W. Ashcroft, *Phys. Rev. A* **15**, 2072 (1977).
  - [17] Y. Rosenfeld, *Phys. Rev. A* **15**, 2545 (1977).
  - [18] Y. Rosenfeld, *J. Phys.: Condens. Matter* **11**, 5415 (1999).
  - [19] H. Ohta and S. Hamaguchi, *Phys. Plasmas* **7**, 4506 (2000).
  - [20] T. Saigo and S. Hamaguchi, *Phys. Plasmas* **9**, 1210 (2002).
  - [21] G. Salin and J. M. Caillol, *Phys. Rev. Lett.* **88**, 065002 (2002).
  - [22] G. Salin and J. M. Caillol, *Phys. Plasmas* **10**, 1220 (2003).
  - [23] J.-P. Hansen and I. R. McDonald, *Theory of Simple Liquids*, 2nd ed. (Academic Press, London, 1986).
  - [24] G. Kalman and K. I. Golden, *Phys. Rev. A* **41**, 5516 (1990).
  - [25] K. I. Golden and G. Kalman, *Phys. Plasmas* **7**, 14 (2000).
  - [26] M. Rosenberg and G. Kalman, *Phys. Rev. E* **56**, 7166 (1997).
  - [27] G. Kalman, M. Rosenberg, and H. E. DeWitt, *J. Phys. IV* **10**, (2000); *Phys. Rev. Lett.* **84**, 6030 (2000).
  - [28] C. A. Iglesias, J. L. Lebowitz, and D. MacGowan, *Phys. Rev. A* **28**, 1667 (1983).
  - [29] C. A. Iglesias, H. E. DeWitt, J. L. Lebowitz, D. MacGowan, and W. B. Hubbard, *Phys. Rev. A* **31**, 1698 (1985).
  - [30] C. A. Iglesias, F. J. Rogers, R. Shepherd, A. Bar-Shalom, M. S. Murillo, D. P. Kilcrease, A. Calisti, and R. W. Lee, *J. Quant. Spectrosc. Radiat. Transf.* **65**, 303 (2000).
  - [31] M. L. Adams, R. W. Lee, H. A. Scott, H. K. Chung, and L.

- Klein, Phys. Rev. E **66**, 066413 (2002).
- [32] H. Ohta and S. Hamaguchi, Phys. Rev. Lett. **84**, 6026 (2000).
- [33] M. S. Murillo, Phys. Rev. Lett. **85**, 2514 (2000).
- [34] Y. Rosenfeld, Phys. Rev. A **46**, 1059 (1992).
- [35] Y. Rosenfeld, Phys. Rev. E **53**, 2000 (1996).
- [36] S. Ogata, H. Iyetomi, and S. Ichimaru, Astrophys. J., Suppl. Ser. **372**, 259 (1991).
- [37] Y. Rosenfeld, Phys. Rev. E **52**, 3292 (1995).
- [38] S. Ichimaru, S. Ogata, and K. Tsuruta, Phys. Rev. E **50**, 2977 (1994).
- [39] F. Lado, Phys. Rev. A **8**, 2548 (1973).
- [40] Y. Rosenfeld and N. W. Ashcroft, Phys. Rev. A **20**, 1208 (1979).
- [41] C. Deutsch, Y. Furutani, and M. M. Gombert, Phys. Rev. A **13**, 2244 (1976).
- [42] Y. Rosenfeld, J. Stat. Phys. **94**, 929 (1998).
- [43] C. Deutsch, Y. Furutani, and M. M. Gombert, Phys. Rep. **69**, 86 (1981).
- [44] F. Lado, S. M. Foiles, and N. W. Ashcroft, Phys. Rev. A **28**, 2374 (1982).
- [45] Y. Rosenfeld, Phys. Rev. A **29**, 2877 (1984).
- [46] F. J. Rogers and D. A. Young, Phys. Rev. A **30**, 999 (1984).
- [47] G. Zérah and J.-P. Hansen, J. Chem. Phys. **84**, 2336 (1986).
- [48] Y. Rosenfeld, J. Stat. Phys. **42**, 437 (1986).
- [49] L. E. Gonzalez, D. J. Gonzalez, and M. Silbert, Physica B **168**, 39 (1991).
- [50] L. E. Gonzalez, D. J. Gonzalez, and M. Silbert, Phys. Rev. A **45**, 3803 (1992).
- [51] H. C. Chen and S. K. Lai, Phys. Rev. A **45**, 3831 (1992).
- [52] K. Hiroike, J. Phys. Soc. Jpn. **12**, 326 (1957).
- [53] L. Verlet and J. J. Weiss, Phys. Rev. A **5**, 939 (1972).
- [54] D. Henderson and E. W. Grundke, J. Chem. Phys. **63**, 601 (1975).
- [55] M. Ross, J. Chem. Phys. **71**, 567 (1979).
- [56] M. S. Wertheim, Phys. Rev. Lett. **10**, 321 (1963); J. Math. Phys. **5**, 643 (1964).
- [57] E. Thiele, J. Chem. Phys. **39**, 474 (1963).
- [58] R. J. Baxter, Aust. J. Phys. **21**, 563 (1968).
- [59] K.-C. Ng, J. Chem. Phys. **61**, 2680 (1974).
- [60] D. Gogny, Nucl. Phys. A **237**, 399 (1975).
- [61] D. Ofer, E. Nardi, and Y. Rosenfeld, Phys. Rev. A **38**, 5801 (1988).
- [62] W. Gautschi, SIAM (Soc. Ind. Appl. Math.) J. Numer. Anal. **7**, 187 (1970).
- [63] K. S. Kölbig, Commun. ACM **15**, 465 (1972).
- [64] W. H. Press, S. A. Teukolski, W. T. Vetterling, and B. P. Flannery, *Numerical Recipes in Fortran: The Art of Scientific Computing*, 2nd ed. (Cambridge University Press, New York, 1992).
- [65] W. Krauth and M. Staudacher, Phys. Lett. B **388**, 808 (1996).
- [66] G. Faussurier, Ann. Phys. (N.Y.) **294**, 203 (2001).
- [67] F. Perrot, Phys. Rev. A **44**, 8334 (1991).
- [68] W. G. Hoover and F. H. Ree, J. Chem. Phys. **49**, 3609 (1968).
- [69] Y. Rosenfeld, Phys. Rev. E **54**, 2827 (1996).
- [70] Y. Rosenfeld, Phys. Rev. A **24**, 2805 (1981).
- [71] J. P. Hansen and L. Verlet, Phys. Rev. **184**, 151 (1969).
- [72] Y. Rosenfeld, Phys. Rev. E **62**, 7524 (2000).
- [73] N. G. Almaraz, E. Lomba, G. Ruiz, and C. F. Tejero, Phys. Rev. E **67**, 021202 (2003).
- [74] C. F. Tejero and M. Baus, J. Chem. Phys. **118**, 892 (2003).
- [75] C. F. Tejero, J. Phys.: Condens. Matter **15**, S395 (2003).
- [76] J.-P. Hansen, I. R. McDonald, and E. L. Pollock, Phys. Rev. A **11**, 1025 (1975).
- [77] Y. Rosenfeld, J. Phys.: Condens. Matter **13**, L39 (2001).
- [78] J. J. Erpenbeck and W. W. Wood, Phys. Rev. A **43**, 4254 (1991).
- [79] J. Wallenborn and M. Baus, Phys. Rev. A **18**, 1737 (1978).
- [80] B. J. Alder, D. M. Gass, and T. M. Wainwright, J. Chem. Phys. **53**, 3813 (1970).
- [81] Z. Donko and B. Nyiri, Phys. Plasmas **7**, 45 (2000).
- [82] B. Bernu and P. Vieillefosse, Phys. Rev. A **18**, 2345 (1978).
- [83] R. Grover, W. G. Hoover, and B. Moran, J. Chem. Phys. **83**, 1255 (1985).
- [84] S. Chapman and T. G. Cowling, *The Mathematical Theory of Non-Uniform Gases* (Cambridge University Press, New York, 1952).
- [85] S. Skupsky, Phys. Rev. A **21**, 1316 (1980).
- [86] S. Torquato, B. Lu, and J. Rubinstein, Phys. Rev. A **41**, 2059 (1990).
- [87] S. Torquato, Phys. Rev. E **51**, 3170 (1995).
- [88] W. G. Hoover and J. C. Poirier, J. Chem. Phys. **37**, 1041 (1962).
- [89] B. Widom, J. Chem. Phys. **39**, 2808 (1963).
- [90] B. Jancovici, J. Stat. Phys. **17**, 357 (1977).
- [91] J. P. Hansen, G. M. Torrie, and P. Vieillefosse, Phys. Rev. A **16**, 2153 (1977).